A NEW ELECTRON SPECTROSCOPY SYSTEM FOR MEASURING ELECTRON EMISSION FROM FAST ION INTERACTIONS WITH ATOMIC, MOLECULAR, AND CONDENSED PHASE TARGETS

By

Wilson L. Hawkins

July 2016

Director of Thesis: Jefferson L. Shinpaugh, PhD

Major Department: Physics

A new electron spectroscopy system has been developed for measuring electron emission from gas and solid targets induced by fast ion impact. This system uses an ultrahigh-vacuum compatible cylindrical deflector analyzer, designed and fabricated in the Department of Physics at East Carolina University, to measure electron yields as a function of electron energy and emission angle for fast ions interacting with materials. The new spectroscopy system was tested in a previously existing high-vacuum target chamber that has been installed on a new beam line in the ECU Accelerator Laboratory. In addition to the new analyzer, a new data acquisition and experimental control system, based on LabVIEW computer control software, was developed and tested using an existing cylindrical mirror analyzer. Data from this system was compared to previous results to confirm the functionality of the design. Subsequently, the new analyzer was installed in the high-vacuum target chamber and tested by measuring Auger electron emission from 2 MeV protons incident on an argon gas target and comparing to well-known emission spectra. Ultimately, the new electron spectroscopy system will be used for measuring electron yields from condensed phase targets in ultrahigh-vacuum conditions in future experiments.

A NEW ELECTRON SPECTROSCOPY SYSTEM FOR MEASURING ELECTRON EMISSION FROM FAST ION INTERACTIONS WITH ATOMIC, MOLECULAR, AND CONDENSED PHASE TARGETS

A Thesis Presented to

the Faculty of the Department of Physics

East Carolina University

In Partial Fulfillment

of the Requirements for the Degree

Master of Science in Applied Physics

By

Wilson L. Hawkins

July 2016

A NEW ELECTRON SPECTROSCOPY SYSTEM FOR MEASURING ELECTRON EMISSION FROM FAST ION INTERACTIONS WITH ATOMIC, MOLECULAR, AND CONDENSED PHASE TARGETS

by

Wilson L. Hawkins

APPROVED BY:

DIRECTOR OF
THESIS: _____
Jefferson L Shinpaugh, PhD

COMMITTEE MEMBER: _____
Regina DeWitt, PhD

COMMITTEE MEMBER: _____
Micheal Dingfelder, PhD

COMMITTEE MEMBER: _____
Robert A. McLawhorn, PhD

CHAIR OF THE DEPARTMENT
OF PHYSICS:_____
Jefferson L. Shinpaugh, PhD

DEAN OF THE
GRADUATE SCHOOL: _____
Paul J. Gemperline, PhD

Acknowledgments

First, I would like to thank my Professor and close friend, Dr. Shinpaugh for his assistance in completing this project. His expertise and experience were vital to overcoming obstacles involved with rebuilding the experiment and understanding the theory of the project.

I would also like to give a special thanks to Mr. Chris Bonnerup for the many hours of help designing the LabVIEW program, providing his electronics expertise, and warming up the ion source at 5am whenever I scheduled beam time.

My appreciation goes out to my committee members Dr. Micheal Dingfelder, Dr. Regina Dewitt, and Dr. Robert McLawhorn for their input and revisions of my paper, insuring a higher quality thesis than I could accomplish on my own.

I would also like to thank my parents, William E. Hawkins Jr. and Anita L. Hawkins. I couldn’t have made it this far in my academic journey without their encouragement and support.

Table of Contents

List of Figures

1 Introduction

1.1 Background

Electron Spectroscopy is an experimental technique in which the energy and angular distribution of electrons emitted from atoms, molecules, or materials are analyzed. Various methods of electron spectroscopy are used in material sciences, atomic physics, space radiation research, and electric propulsion to measure the energy and angular distribution of emitted electrons [1, 2]. The objective of this project was to develop a new electron spectroscopy system for measuring high-energy electrons (>50 eV) that can be used in an ultrahigh-vacuum system to complement current low-energy electron measurements at ECU [3, 4].

In 2009, a National Science Foundation grant was awarded to Dr. Jefferson Shinpaugh and Dr. Larry Toburen at East Carolina University for the purchase of a new particle accelerator. In light of this award, ECU offered to renovate the current space to accommodate the new machine. This renovation involved the decommissioning and replacement of the old 2 MV Van de Graaff particle accelerator with a new 2 MV tandem Pelletron particle accelerator. All equipment including target chambers, electronics, and tools were moved off site into storage for construction purposes. Reconstructing the lab after the delivery of the new accelerator gave us an opportunity to upgrade many experimental systems. A target chamber designed and used by Dr. Toburen and Dr. Shinpaugh to measure electron emission cross sections from gas targets was recommissioned after the 2011 renovation of the ECU Accelerator Lab during the initial phase of this project. A Computer Automated Measurement and Control (CAMAC) data acquisition system was replaced by a National Instruments USB controller, controlled by a new LabVIEW

software program. The next project for this experiment was the testing of a new type of electrostatic analyzer designed by Dr. Robert McLawhorn prior to the renovation. This project includes the instrumentation upgrade of the electron spectroscopy system previously employed.

1.2 Electrostatic Analyzers

In the most common method of electron spectroscopy, an electrostatic analyzer is used to deflect the path of the electron's trajectory using an electric field. Based on the strength of the electric field and the ESA's geometry, only electrons of a specific energy are directed out of the ESA's exit aperture. At the exit aperture, a detector is positioned to collect the electrons. The detector signal is amplified and transferred to a data acquisition system which counts the number of pulses using a data acquisition system controlled by a computer. In chapter 2, an overview of the new data acquisition system used for this experiment is presented.

An electric field is produced inside of the ESA using an applied voltage across two plates. This applied voltage, along with the geometry of the analyzer, defined by its "geometric constant" (also referred to as the spectrometer constant), determines the allowed electron transmission energy to escape the exit aperture [1, 2, 5, 6]. The relationship between the applied voltage V, transmission energy E per unit charge q, and the geometric constant C is

$$V = \left(\frac{E}{q}\right) C. \tag{1}$$

The simplest ESA is the plane mirror analyzer (PMA), shown in Fig. 1.1. Two parallel, planar plates are positioned a certain distance apart with one plate designed to pass electrons with an entrance angle of 45° through entrance and exit apertures [2]. The plate opposite of the aperture plate is biased negatively to create a retarding field, which deflects incoming electrons to alter the electron's trajectory. If the energy of an incoming electron is too large, it will overshoot the exit aperture, thus not being detected outside of the analyzer. For lower energy electrons, relative to the transmission energy, they will undershoot the exit aperture resulting in the inability to escape the analyzer. The geometric constant C for a simple PMA,

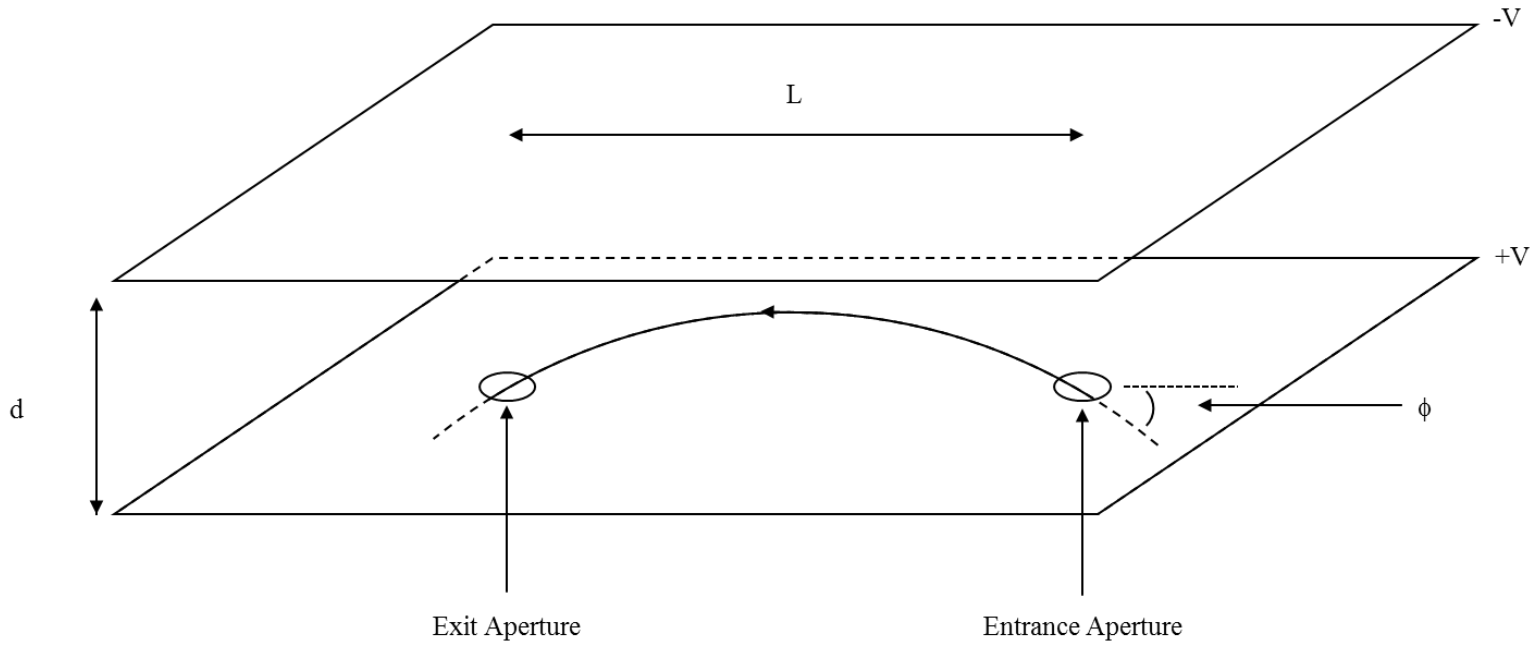

FIG 1.1 Diagram of a plane mirror analyzer.

$$C = 2\left(\frac{d}{L}\right) \tag{2}$$

can be calculated using the ratio of inner plate separation distance *d* to the focusing distance *L* [2]. Thus, in order to make the geometric constant 1, the plate separation must be half of the focusing distance. This is sometimes desired experimentally, in order to know there is a 1:1 correspondence between applied voltage and transmission energy per charge. This separation distance to focusing distance ratio is possible because the maximum trajectory height *X* at an entrance angle of 45° for selected electrons is

$$X = \frac{L}{4} \tag{3}$$

as shown by Roy and Tremblay [6].

The cylindrical mirror analyzer (CMA) is a unique type of parallel plate analyzer designed with two cylindrical plates of different radii sharing a common central axis [2, 6]. The inner plate is grounded and fitted with two apertures allowing electron transmission, while the outer plate is negatively biased to create a retarding field similar to the PMA. A diagram of a CMA is shown in Fig. 1.2. The advantage a CMA has over a PMA involves the added focusing perpendicular to the plane of deflection [1, 2, 6]. This additional perpendicular focusing allows a larger azimuthal acceptance angle thus leading to higher efficiency. Unlike a PMA, the CMA's focusing distance is measured as the distance between the entrance and exit points of the electron trajectory along the axis of symmetry instead of the inner plate's aperture separation distance. The entrance aperture is set to an entrance angle of 42.3°, where first order focusing occurs for CMA geometry [1]. For this entrance angle, the relationship between the focusing length L and inner plate radii r_1 is $L = 6.13r_1$. With this relationship, the geometric coefficient C for a CMA

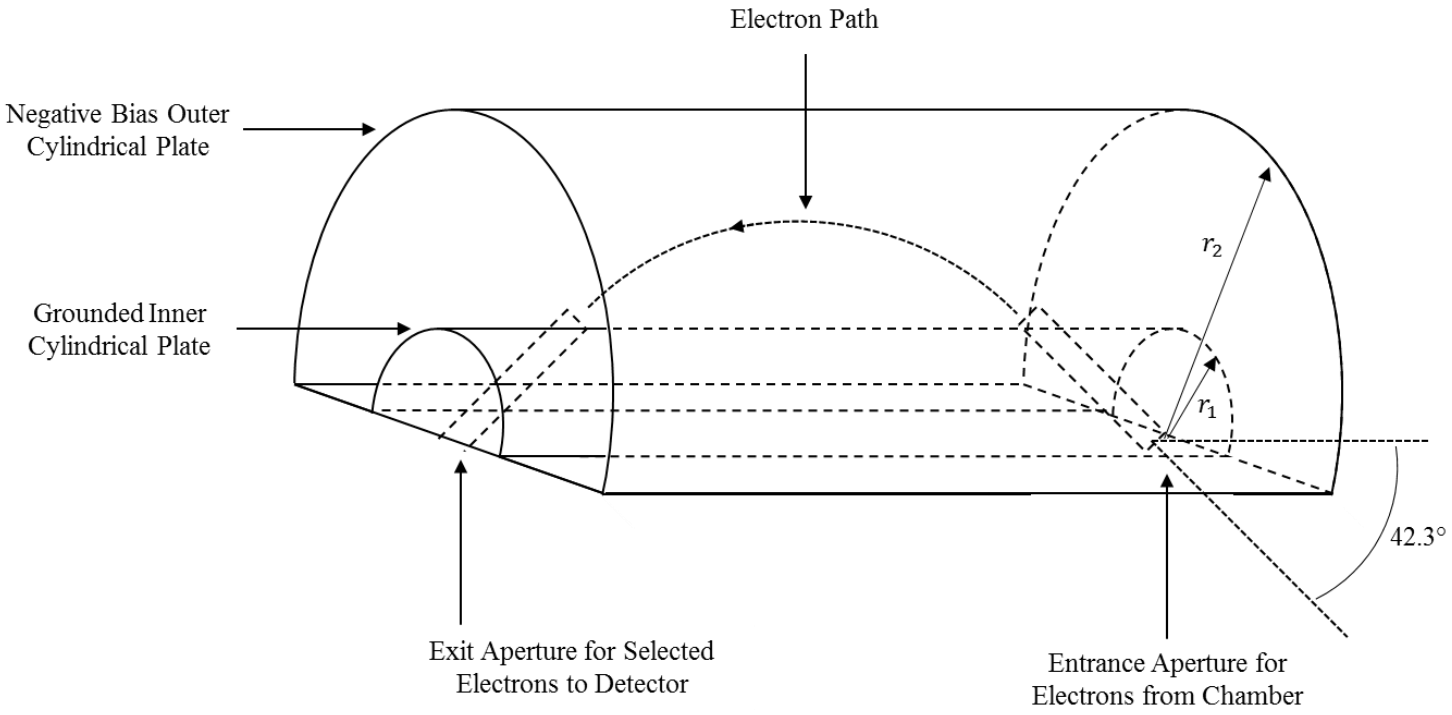

FIG 1.2 Schematic of a cylindrical mirror analyzer. Electrons enter the entrance aperture from the right and are repelled away from the negatively biased outer plate into the exit aperture on the left, where they are detected.

$$C = 0.763 \ln\left(\frac{r_2}{r_1}\right) \tag{4}$$

can be written in terms of the ratio of outer r_2 to inner r_1 plate radii [6]. In order to achieve a geometric constant of 1, the inner and out radii must be related by $r_2 = 3.708 r_1$. Since the maximum radial component of the electron trajectory X has been shown to be $X = 1.8 r_1$, this inner to outer radius ratio is attainable [2].

The cylindrical deflector analyzer (CDA) is another type of parallel plate analyzer that while having no focusing in the transverse plane of travel, offers higher energy resolution with a unique geometry [1, 2, 6]. A diagram of a CDA is shown in Fig. 1.3. The inner plate of the CDA is biased at a positive voltage V_1 with an outer radius of r_1 and the outer plate is biased at a negative voltage V_2 with inner radius r_2. CDA's can be designed in such a way that the inner and outer plates are set to equal and opposite voltages $V_1 = -V_2$ which forces the electron path radius r_0 to be defined by $r_0 = \sqrt{r_1 r_2}$ [2, 7]. The geometric coefficient of a CDA,

$$C = \left(2 \ln\left(\frac{r_2}{r_1}\right)\right) \tag{5}$$

is determined by the inner plate's outer radius r_1 and the outer plate's inner radius r_2 [1, 2, 6]. The geometry of the electric field inside of the CDA generates first order focusing at a characteristic 127.3° angle of travel for electrons [1, 7].

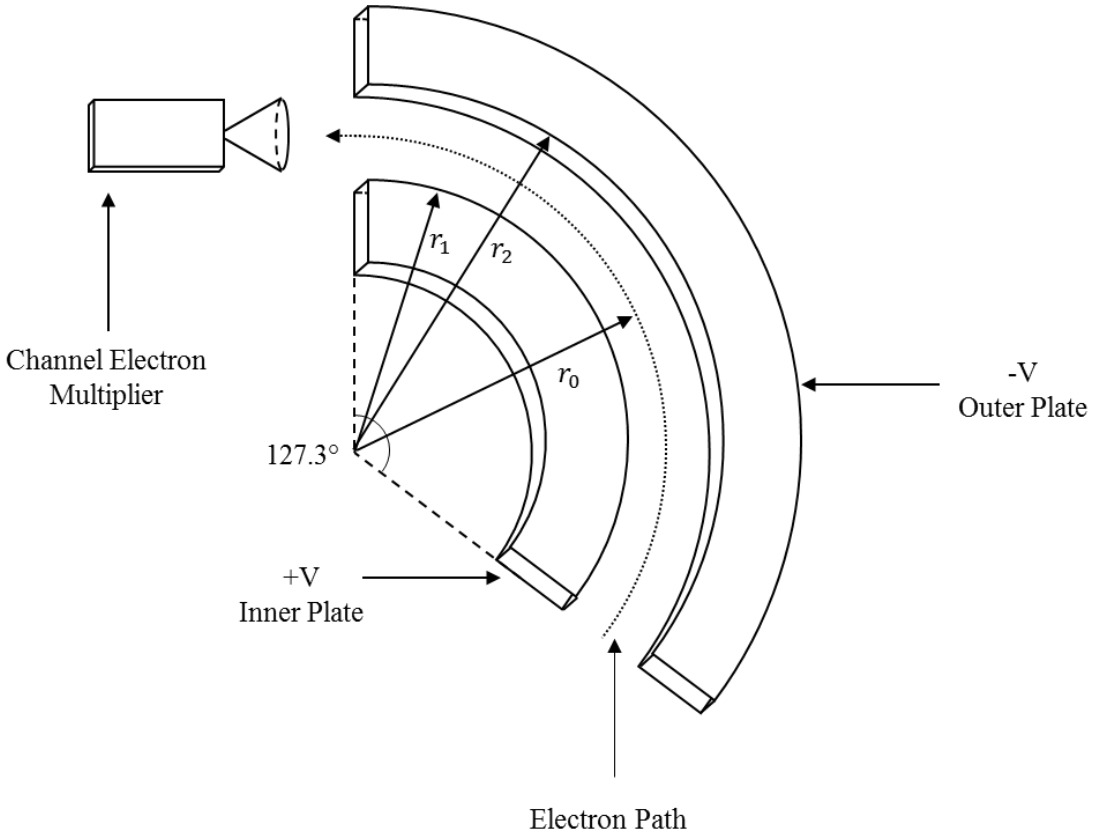

FIG 1.3 Diagram of a cylindrical deflector analyzer. Electron path and separate channel electron multiplier shown.

1.3 Auger Electron Emission

Investigation into the subatomic properties of matter has played a vital role in our understanding of the universe. This knowledge leads to practical applications in technology, medicine, engineering, and many other fields of study. In order to understand interactions on an atomic or subatomic scale, information about subatomic structure is needed. Around the turn of the 20^{th} century, an understanding of electromagnetic waves, or photons, allowed scientists to obtain information about atomic structure in the form of photon emission from de-excitation of atoms [8]. Over the next 100 years, technological advances have allowed for a variety of methods in extracting information about atomic structure. One of these methods is the capture of electrons emitted from collision interactions between various particles, atoms, and ions [9]. Emitted electron kinetic energy and angular scattering offer insight into the substructure of the material to which they were bound. One of the many mechanisms through which an electron can be ejected from a material is through the Auger-electron emission process [10].

During an interaction with a fast ion, for example, energy can be transferred to the electrons of an atom [9]. If this energy is given to an electron in an inner shell, this electron can be ejected from the atom, creating a vacancy [11]. This vacancy allows for the acceptance of an electron in a higher energy state in an outer shell to move to a preferred lower energy state without being in violation of the Pauli Exclusion Principle. This excess energy must be conserved in the form of energy transfer or photon emission. Auger-electron emission is a mechanism by which an outer shell electron is ejected from an atom by receiving this excess energy [11]. A diagram illustrating the Auger-electron emission process is shown in Fig. 1.4. Each element on the periodic table has, by definition, a unique configuration and number of subatomic particles. Consequentially, each element has a unique nuclear, atomic, and electron

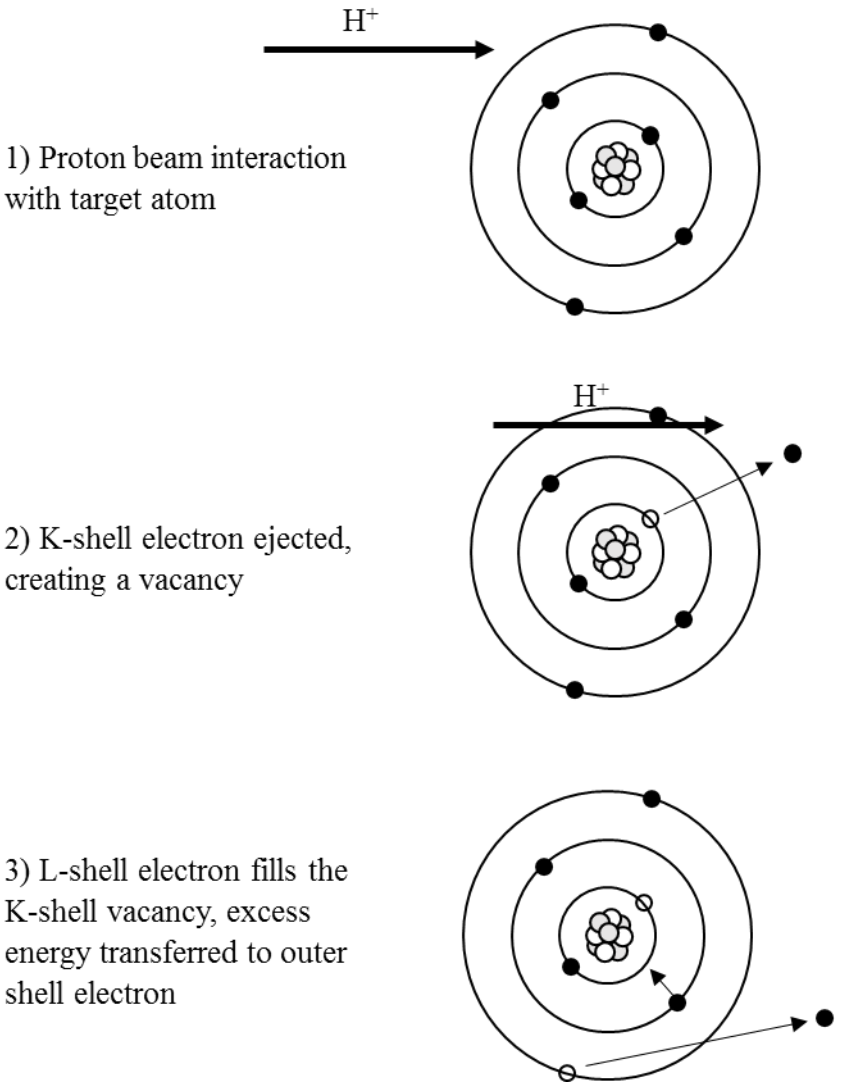

FIG 1.4 Diagram of the Auger electron emission process.

cloud structure [12]. This causes unique energy gaps between electron orbitals [12].

For the experiments in this paper, well-known K-shell Auger-electron detection was used to verify the correct operation of the new spectroscopy system. This is a useful tool in determining the accuracy of an ESA's geometric coefficient at different energy ranges by dividing the analyzer voltage value at the Auger peak by the known Auger-electron energy value.

2 Materials and Methods

2.1 Accelerator Lab

Ions were produced by a high-intensity General Ionics Corporation cesium sputter ion source, the design of which was first developed by Dr. Roy Middleton in 1982 [13]. A basic diagram of the ion source is shown in Fig 2.1. This ion source uses an insulated heater to bake a reservoir of solid cesium metal to a temperature of roughly 60 °C, which releases Cs vapor into the ion source chamber containing an ionizing heated coil, referred to as the ionizer, and a cathode biased at -7.5 kV [13]. This chamber is heated to approximately 1100 °C during operation of the source. The cathode material used was a titanium hydride (TiH_2) filled copper cylindrical chamber (the "cathode") that attracts the Cs^+ plasma, causing a variety of sub molecular species to be ejected off of the TiH_2 in the form of sputtering [14]. Of these ejected particles, the negatively charged ions are then accelerated through a potential of 30 kV downstream towards a selecting magnet. The inflection magnet was calibrated such that the only species passing though were H^- ions. After the negatively charged ions are accelerated toward the centrally located 1 MV terminal, a N_2 stripper gas is used to shed the ions of their electrons, making them single protons, H^+. This change in species results in a repelling of the positively charged ions away from the centrally located 1 MV terminal, thus leading to a dual acceleration, with the result being a 2 MeV proton beam. Due to this double acceleration via electron stripping, the 2 MV accelerator can accelerate protons to 4 MeV.

National Electrostatics Corporation manufactured the 2 MV tandem Pelletron accelerator used for these experiments. The general setup of the accelerator lab system is shown in Fig. 2.2.

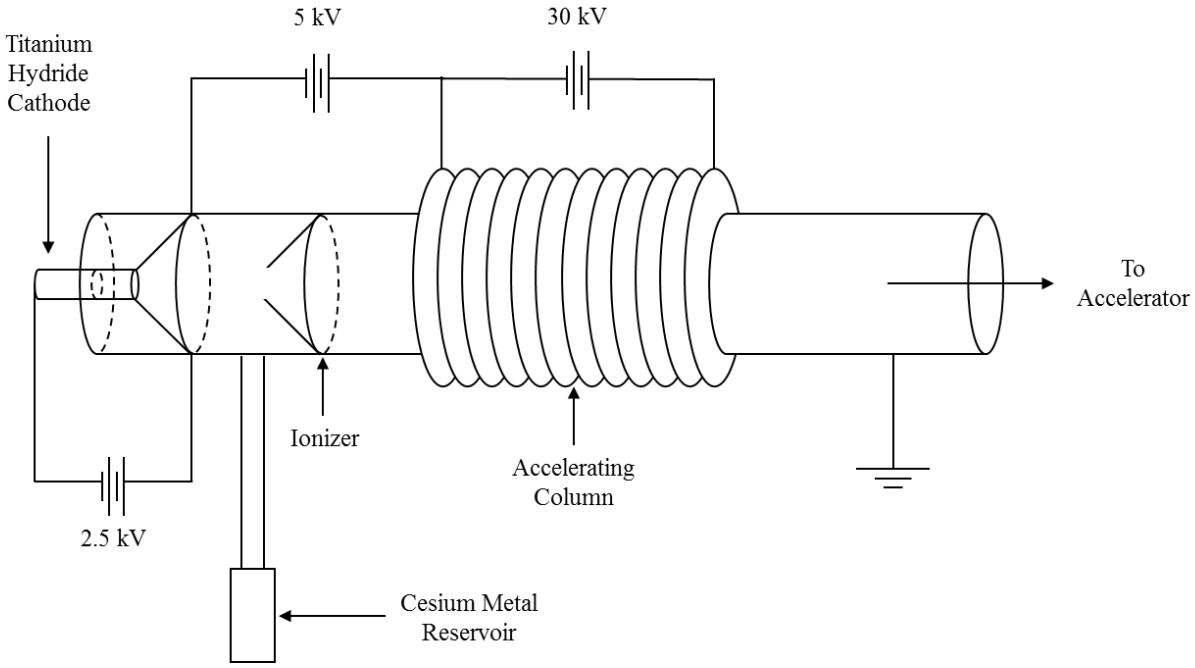

FIG 2.1 Ion Source used to produce ions for the ECU Accelerator Lab. Solid Cesium is heated to a plasma state before bombarding the high Z material filled cathode on the left. Negatively charged ions sputtered off the cathode are accelerated to the right.

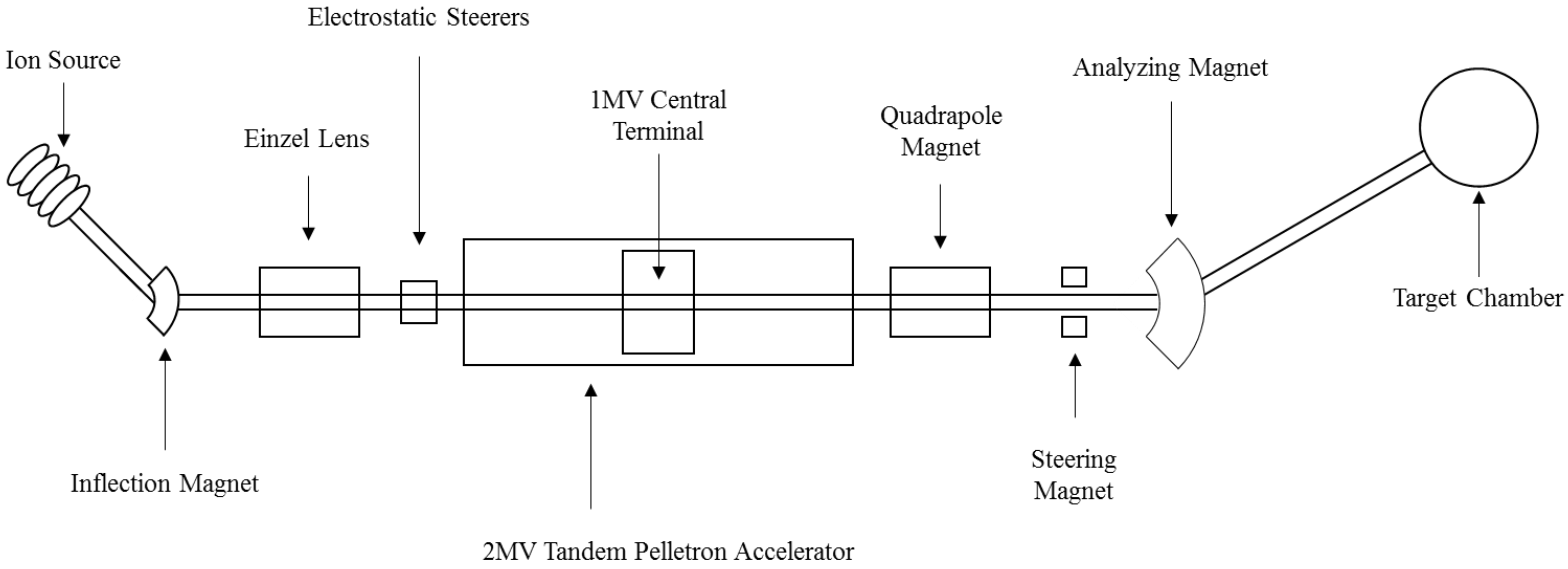

FIG 2.2 View from above of the ECU accelerator laboratory.

An isolated vacuum-sealed beam line is centered in the accelerator tank to allow passage of various ions. A central terminal is charged using a charge carrying chain system to establish up to a 2 MV potential with respect to the 0 V entrance and exit regions. This charge carrying procedure is similar to the way a Van de Graff generator works. In order to create a uniform accelerating field, a series of high voltage plates are located on either side of the central terminal that step the voltage of the central terminal down to the entrance and exit sides of the tank. Sulfur hexafluoride insulating gas surrounds the vacuum-sealed beam line in the accelerator tank to prevent discharging of the high voltage plates. After the beam exits the accelerator tank a quadrupole magnet is used for beam focusing, an "up/down" magnet is used to steer the beam vertically, and an analyzing magnet steers the beam into one of the seven possible beam lines. Faraday cups are positioned before and after the accelerator tank as well as in each beam line in order to monitor the beam at each stage, optimizing the shape of the beam and maximizing transmitted beam current. Quartz crystals were used to monitor the shape of the beam spot through fluorescence at several locations along the beam path. The entirety of the beam line from ion source to target chamber must be under high-vacuum in order to not interrupt the ion beam trajectory. This is achieved by the use of several turbomolecular pumps along the beam line that maintain pressure of approximately 10^{-7} Torr in the system.

A diagram of the beam line used to transport proton beam to the target chamber is shown in Fig 2.3. Gate valves were used to isolate the experimental beamline from the accelerator and target chamber. A Faraday cup was placed in the experimental beam line to maximize the beam current prior to beam on target maximization in the target chamber. The beam was collimated by adjustable 4-jaw slits and a circular collimator located in the target chamber. A quartz viewer was used to monitor the beam profile when optimizing beam transmission through the beamline.

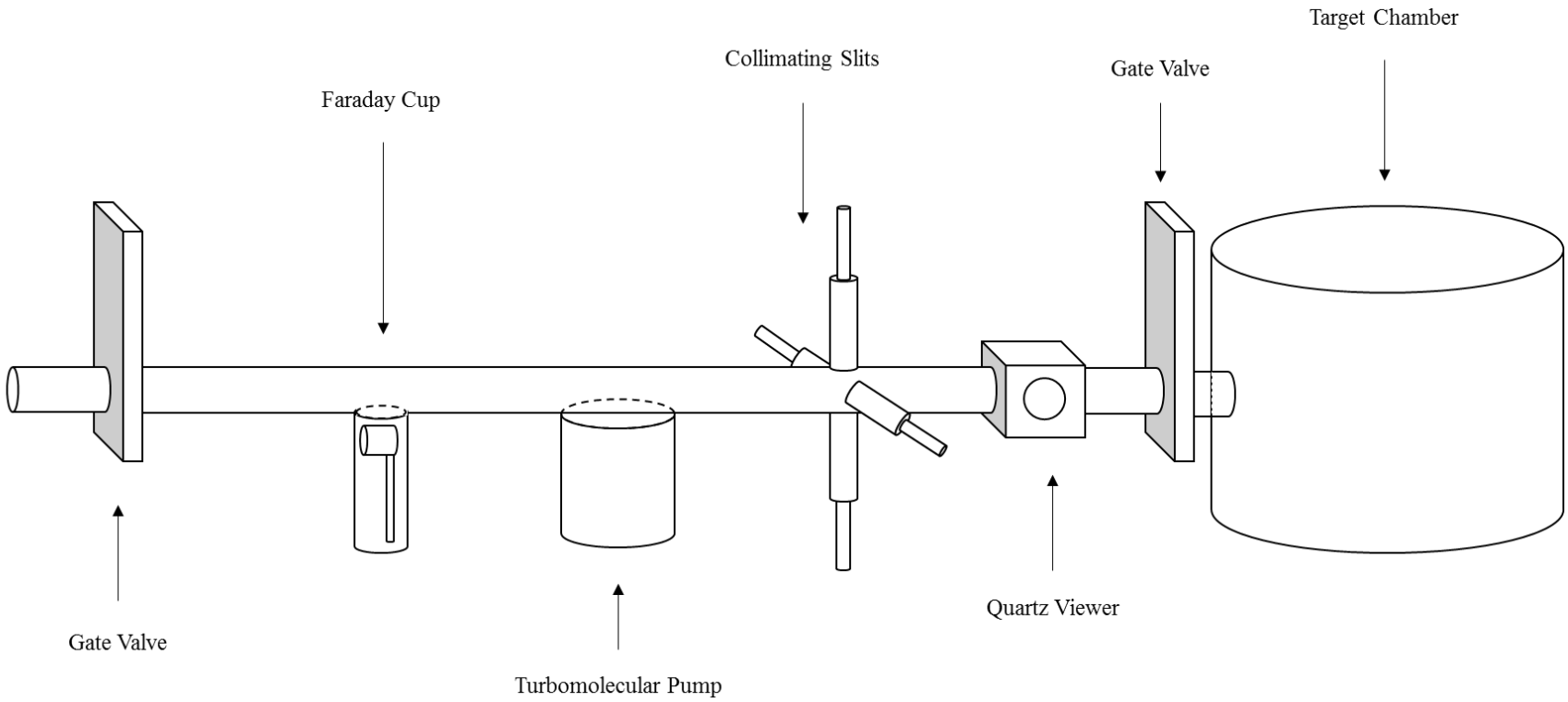

FIG 2.3 Diagram of the experimental beam line between the target chamber and accelerator.

2.2 Target Chamber

The high-vacuum target chamber used for this experiment was specifically designed for measuring scattered electrons from gas targets. A diagram of the target chamber is shown in Fig. 2.4. A two-stage collimator is positioned onto the entrance of the target chamber to achieve a collimated 5mm diameter beam on target. After the proton beam travels through the chamber it is collected in a Faraday cup in the back of the chamber in order to record the number of incident protons on the target gas during data acquisition. The target gas is injected into the chamber vertically downward through a collimated holes structure in the center of the chamber using a MKS Baratron Type 121A absolute pressure transducer to monitor the "pushing" pressure. A high volume diffusion pump provides a vacuum pressure of roughly 10^{-6} Torr without the target gas and 10^{-5} Torr with the gas present. An adjustable arm connected to the center of the chamber and the analyzer determined the angle of the analyzer entrance aperture relative to the incident protons. This angle was measured using a 1 kΩ 270-degree linear potentiometer. The angular range over which electrons were collected for this experiment was 45-90 degrees from the incident proton beam. Assuming azimuthal symmetry of scattered electrons with respect to the proton beam, only one plane needs to be analyzed to know information about the total solid angle scattering. A large double walled container made of magnetic shielding material encases this target chamber in an attempt to negate the effect of external magnetic fields altering the trajectory of electrons.

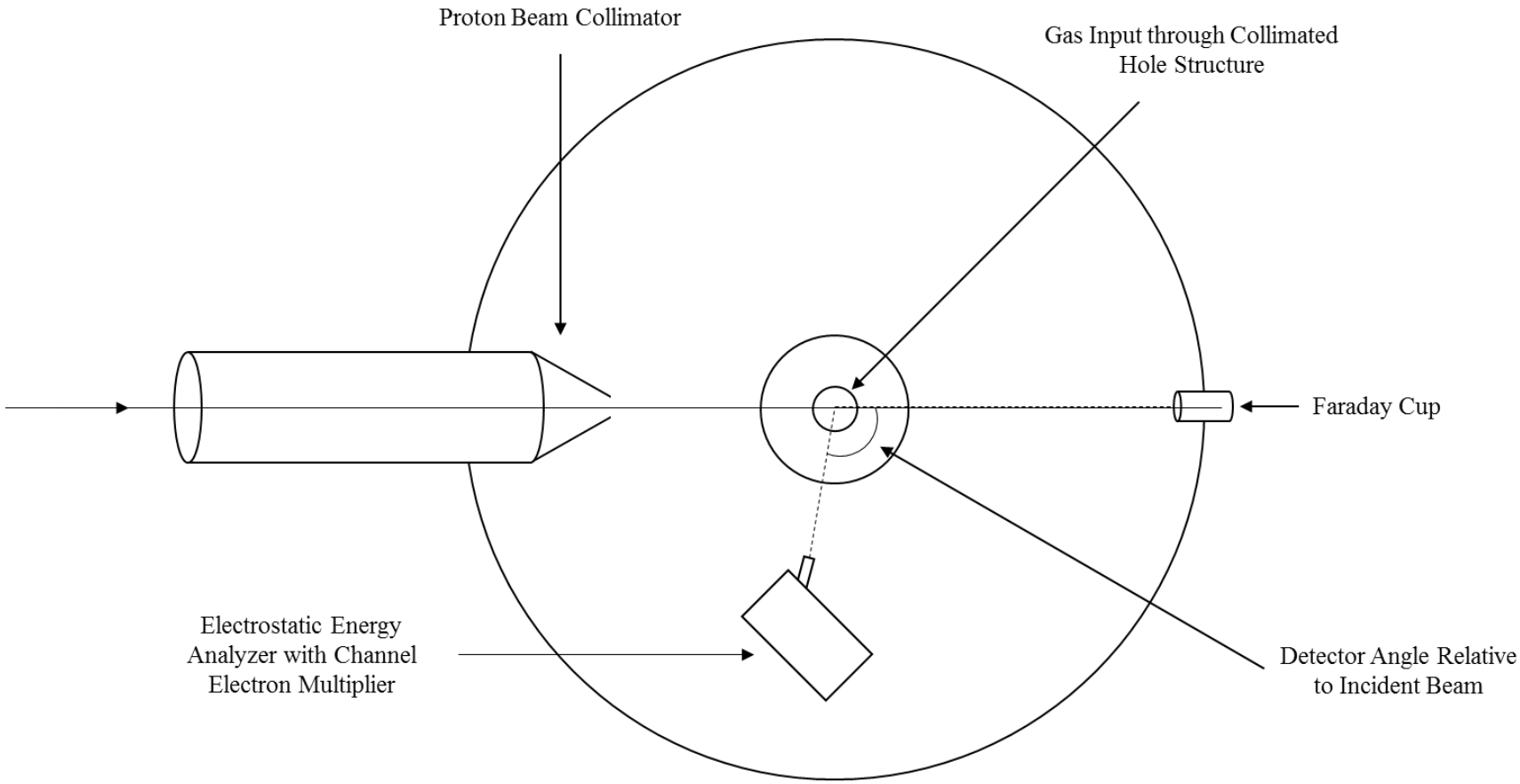

FIG 2.4 Schematic of the target chamber used for measuring emitted electrons from gas targets. The incident beam enters the chamber from the left and is collected in a Faraday cup.

2.3 Data Acquisition System

A new data acquisition system was designed to replace the previously used CAMAC based data acquisition system. This includes the use of a single National Instruments USB X Series instrument that replaced the need for a series of NIM modules. This new system eliminates a series of problems including the compounding error associated with multiple NIM modules and offers a low power alternative that includes new built-in functions including error messages and more precise signal controls.

The main goal when building the new data acquisition system was to simultaneously measure the number of protons incident on a target gas and the number of electrons detected by the channel electron multiplier that pass through an analyzer at a given analyzer plate voltage. A basic diagram of this data acquisition system is shown in Fig. 2.5. The main components of this data acquisition system are a proton counting current integrator, an electron counting channel electron multiplier powered by a high voltage supply coupled with a signal amplifier and discriminator, and a high voltage supply for the analyzer plates.

A Brookhaven Instruments Corporation (BIC) designed current integrator is connected to the Faraday cup in the back of the target chamber. The current integrator stores up charge on a capacitor until a certain criteria is met, then discharges and sends an output signal to the USB controller. This allows for a direct measure of the number of protons collected by the Faraday cup in the form of measuring stored charge. The BIC has an adjustable full range scale that is set by the user on the face of the current integrator in the electronics rack. The BIC is designed to output 1000 signal pulses at full range.

A Dr. Sjuts channel electron multiplier (CEM) was installed in each analyzer used to count the electrons of the analyzer-determined pass energy. The diagram of the CEM is

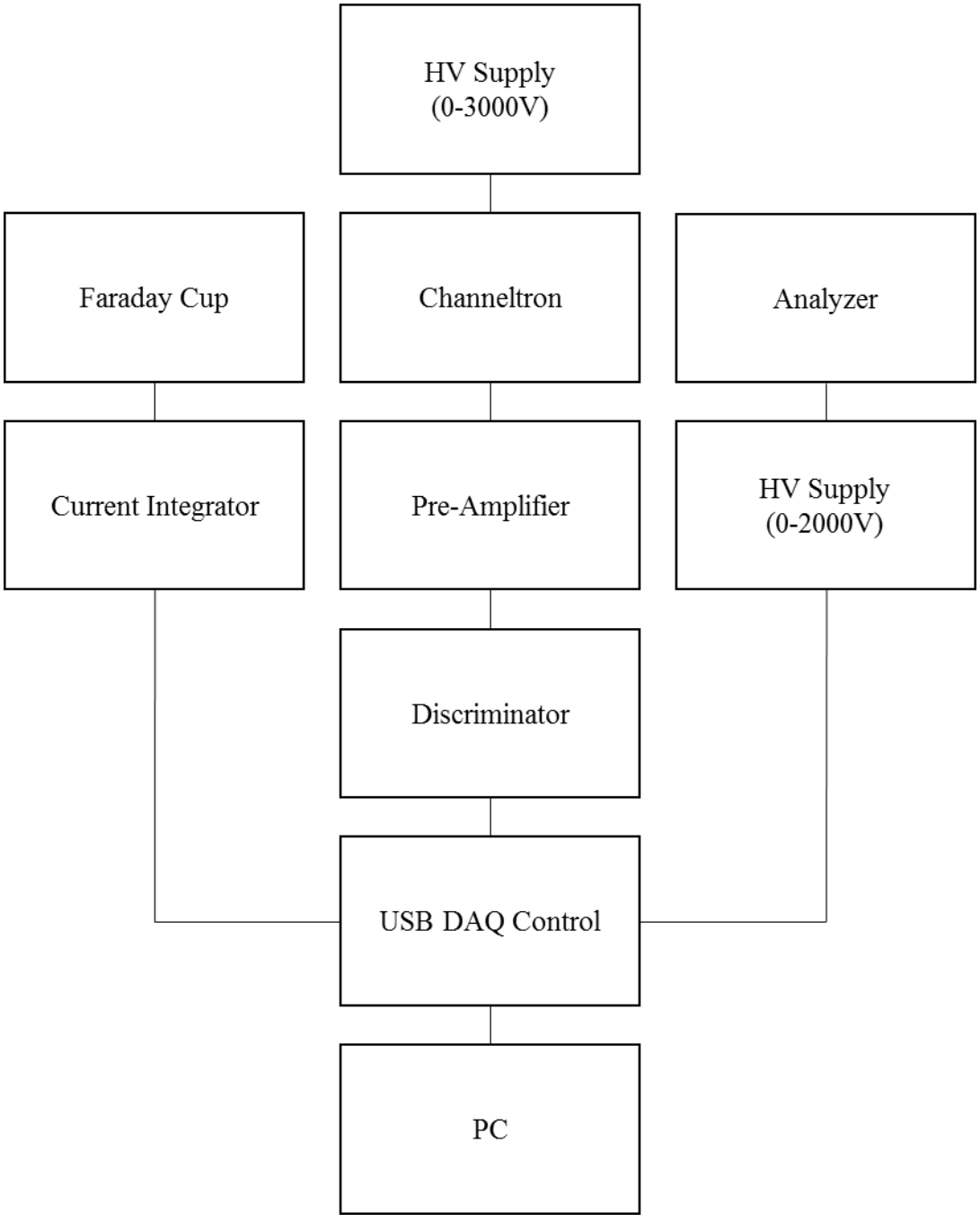

FIG 2.5 Simple diagram of the data acquisition system. Simultaneously measures protons from the incident beam and scattered electrons from the target gas using a PC controlled USB connected board.

shown in Fig. 2.6. The CEM uses a 0-3000 V high voltage power supply to establish a positive bias used to attract electrons through a cascading apparatus similar to a photomultiplier tube. The voltage set on the CEM is a static voltage that remains unchanged throughout data collection. For the experiments of this project, the CEM was set to 2.5 kV. The CEM was equipped with a voltage divider and capacitive pick-off in order to create an output pulse for each incident electron. The CEM has a gain of approximately 10^6 and generates a negative pulse signal of about 100 mV in amplitude. This 100 mV signal is then relayed to a signal amplifier which was set to amplify the signal by six times, resulting in a negative 600 mV pulse. This 600 mV pulse is then relayed to a discriminator set to filter out all signals less than 500 mV and output a positive square wave digital pulse. This positive pulse is then sent to the USB controller to be counted, corresponding to a single analyzed electron.

A 0-2000 V high voltage power supply was connected to both the analyzer in use and the USB controller to hold the analyzer plates at desired voltages. The range of this high voltage power supply is 0-2000 V and is controlled by the PC via the USB controller. This power supply has two controllable outputs, which were utilized for the use of the CDA to simultaneously bias both plates. A 0-10 V digital signal is sent from the USB controller setting the high voltage power supply to a corresponding 0-2000 V. An additional read out of the actual voltage applied across each analyzer plate is monitored by the USB controller in a similar way by reading a 0-10 V signal from the high voltage power supply corresponding to 0-2000 V actual voltage.

The PC that controls the USB controller is equipped with a new LabVIEW program that consists of a user interface shown in Fig. 2.7 and a block diagram shown in Fig. 2.8-12. This program was designed to receive an input Comma Separated Variable (CSV) file containing a table of numbers corresponding to the desired voltage steps of the analyzer plates and

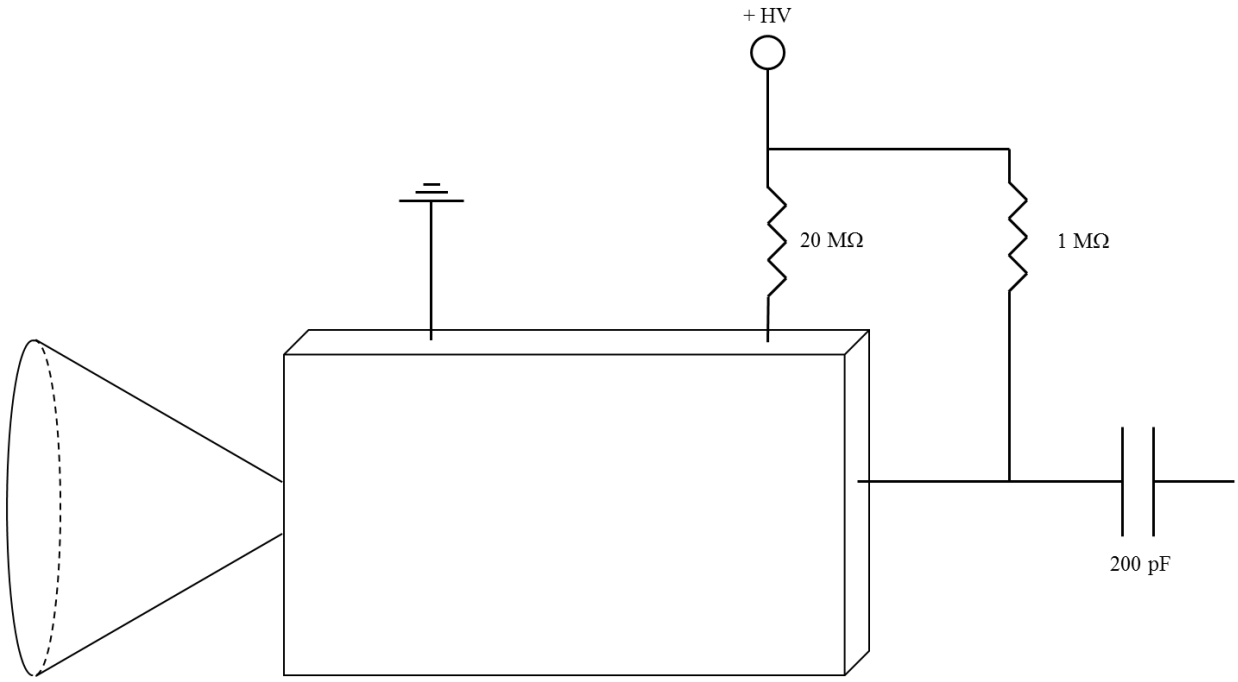

FIG 2.6 Electronic schematic of Channel Electron Multiplier used in both analyzers. A positive bias is applied to the back of the CEM to attract electrons through the cascading apparatus. Voltage divider and capacitive pick-off shown on the right.

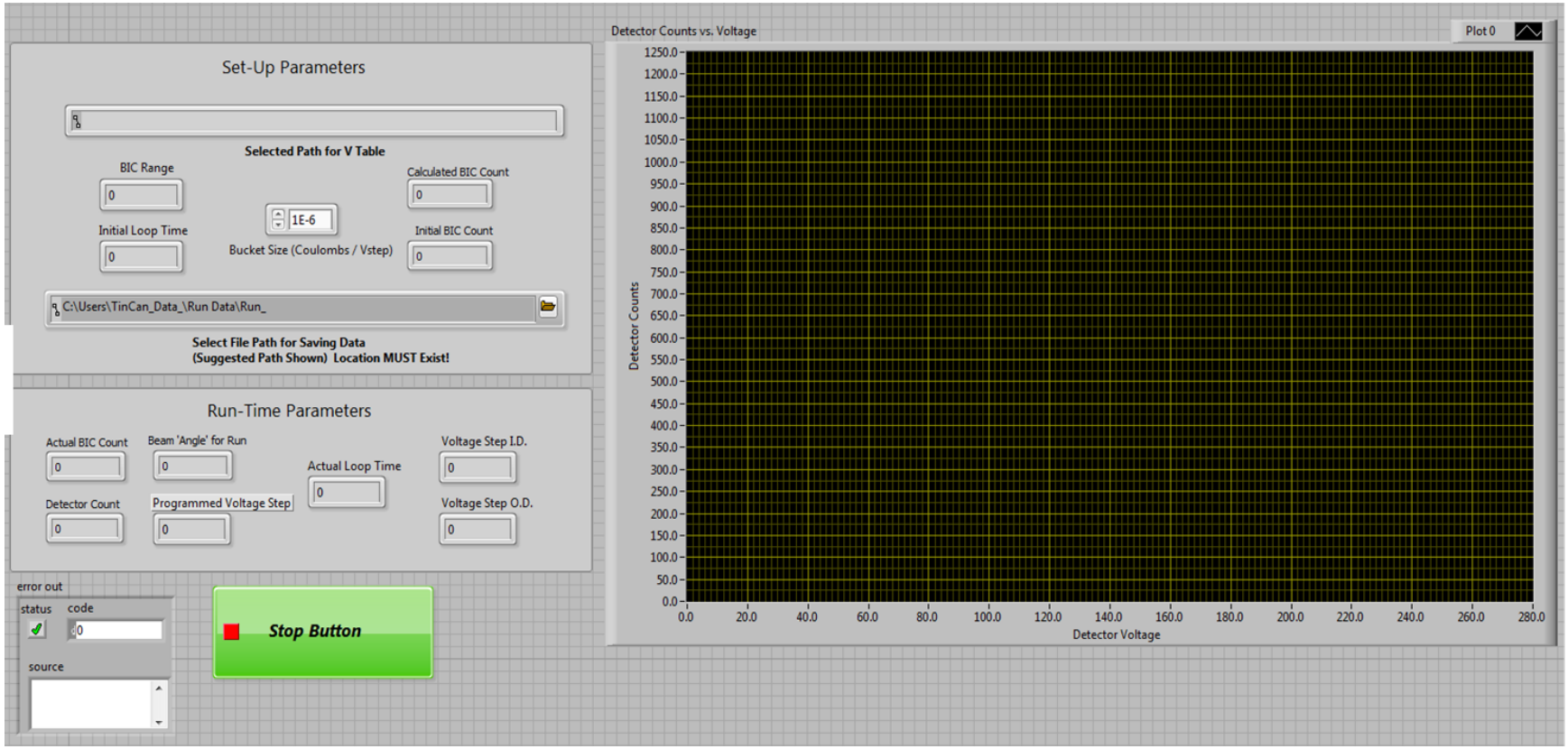

FIG 2.7 User interface of the LabVIEW program. The set-up parameters window displays the settings for the BIC current integrator and output file save location. The run-time parameters window shows in real time updated information about the current voltage step. A real-time 2D plot of electron counts vs. analyzer voltage is displayed and updates after each voltage step.

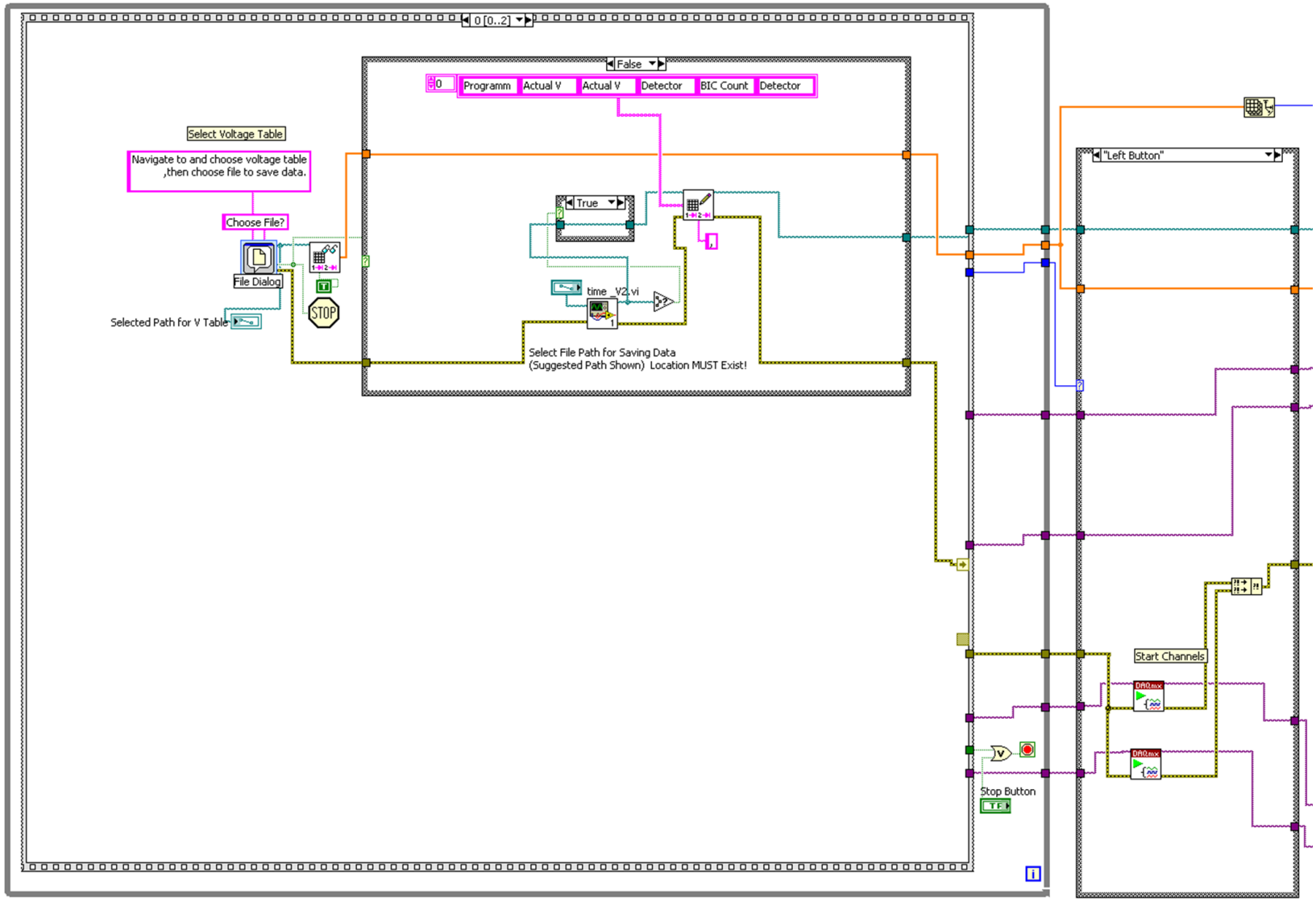

FIG 2.8 Block diagram of the LabVIEW set-up loop with the first task of the inner loop displayed. This inner loop task formats the user interface window.

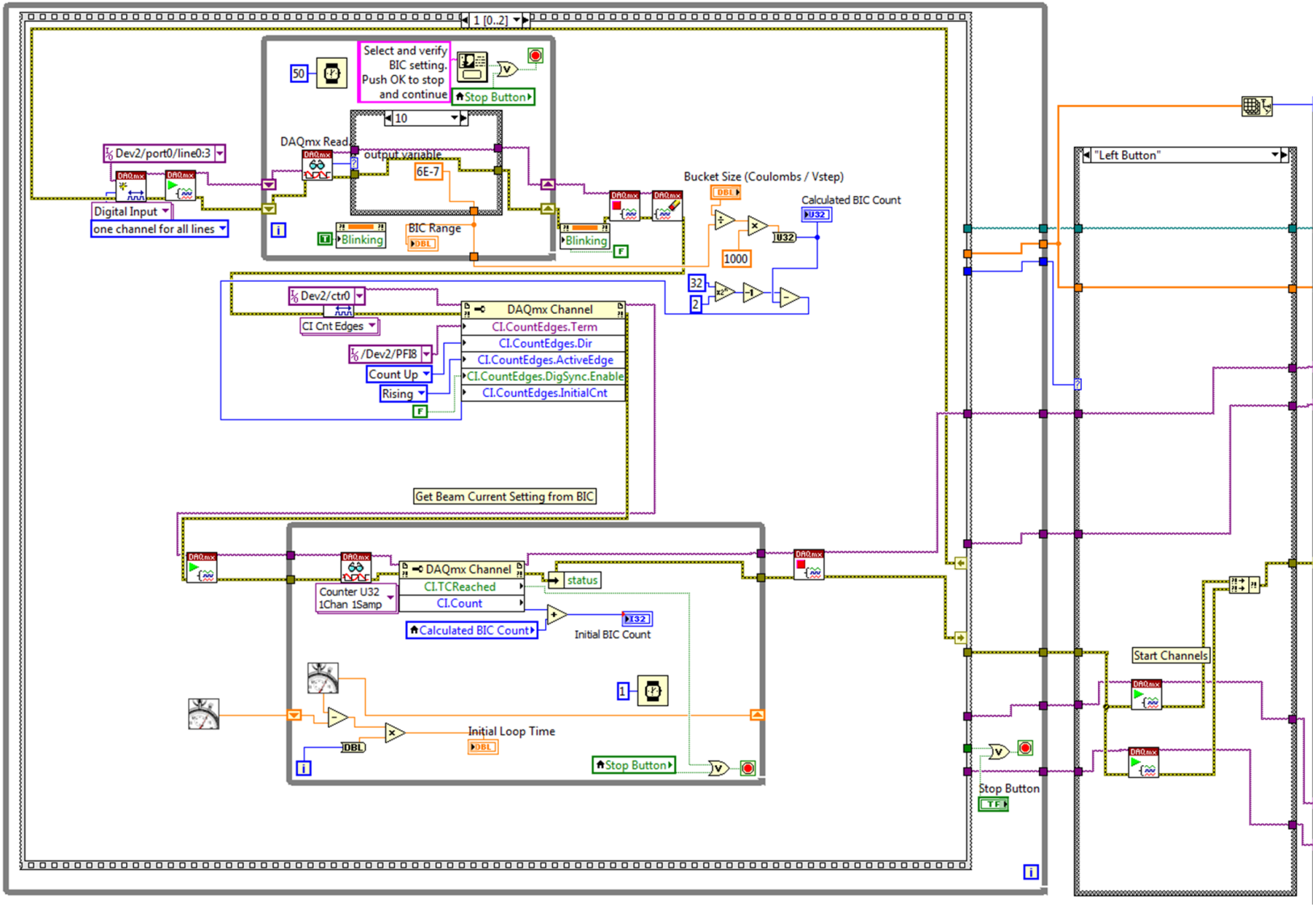

FIG 2.9 Block diagram of the LabVIEW set-up loop with the second task of the inner loop displayed. This task programs the settings for proton counting using the BIC.

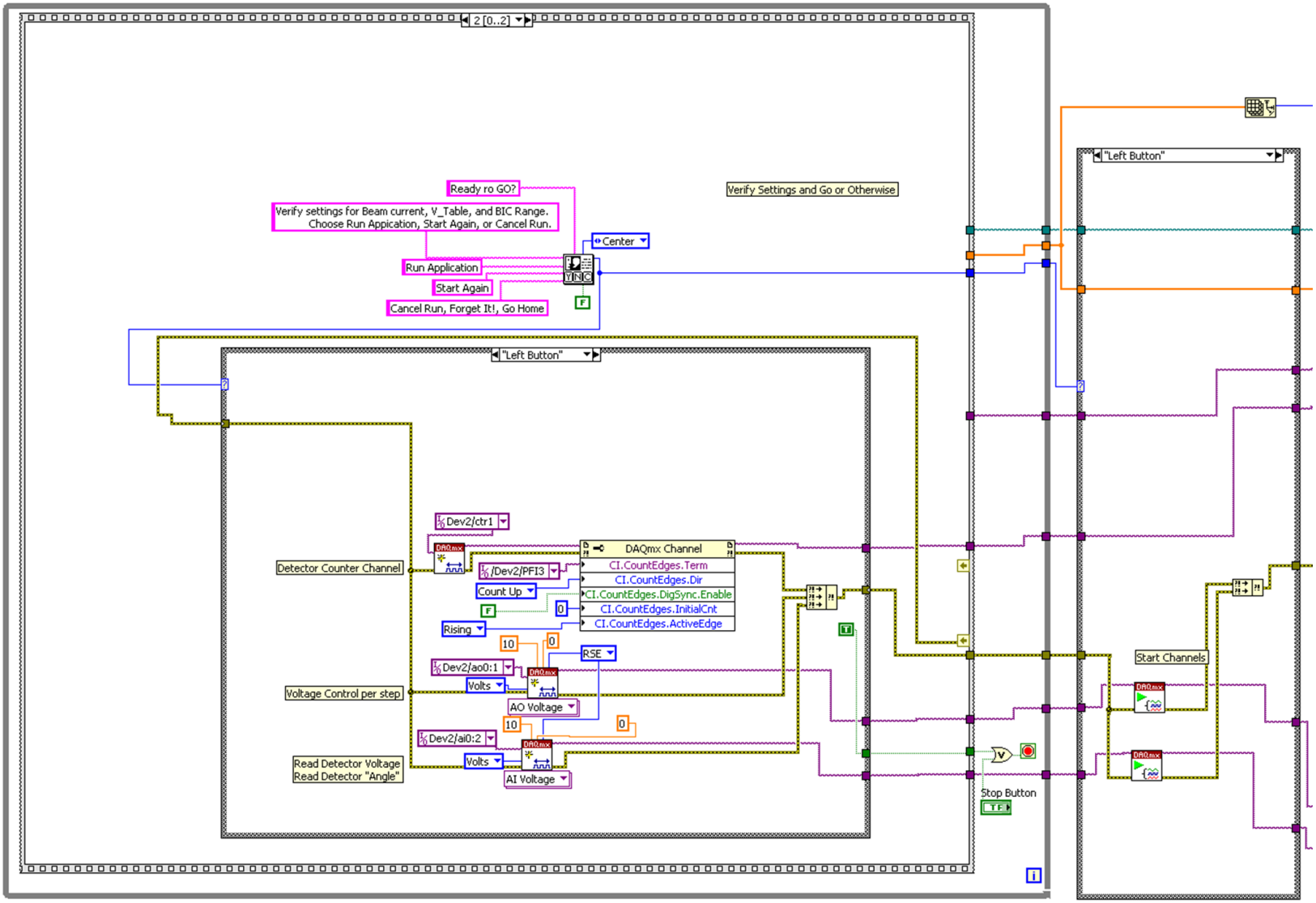

FIG 2.10 Block diagram of the LabVIEW set-up loop with the third stage of the inner loop displayed. This task programs settings for electron counting using the discriminator input signals.

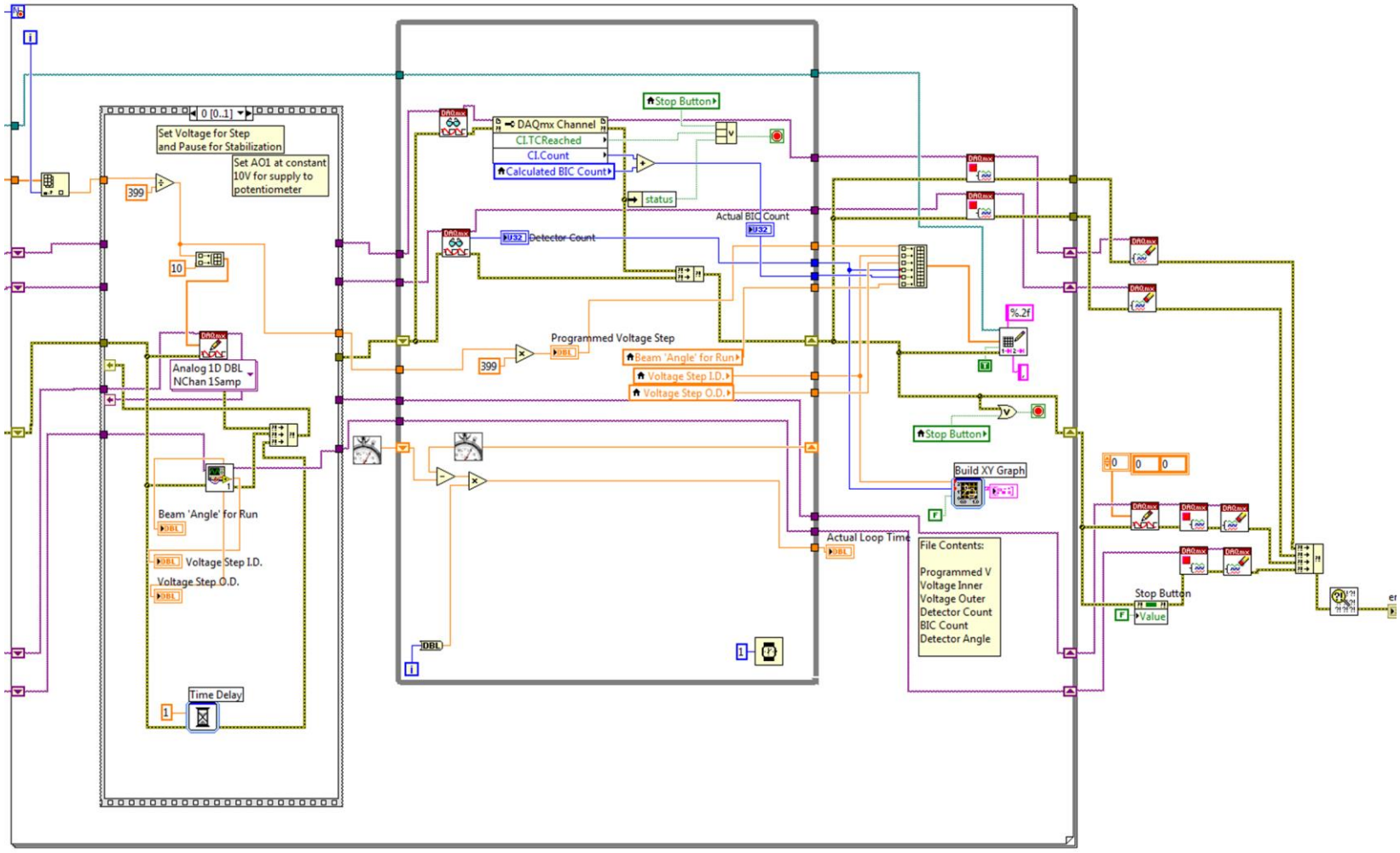

FIG 2.11 Block diagram of the LabVIEW run time loop with the first inner loop task displayed. This task defines the current voltage step and detector angle while reporting the actual voltages of each analyzer plate. The second inner loop iterates each time a count signal is received from the BIC. This loop constantly updates displayed BIC count, detector count, and actual loop time.

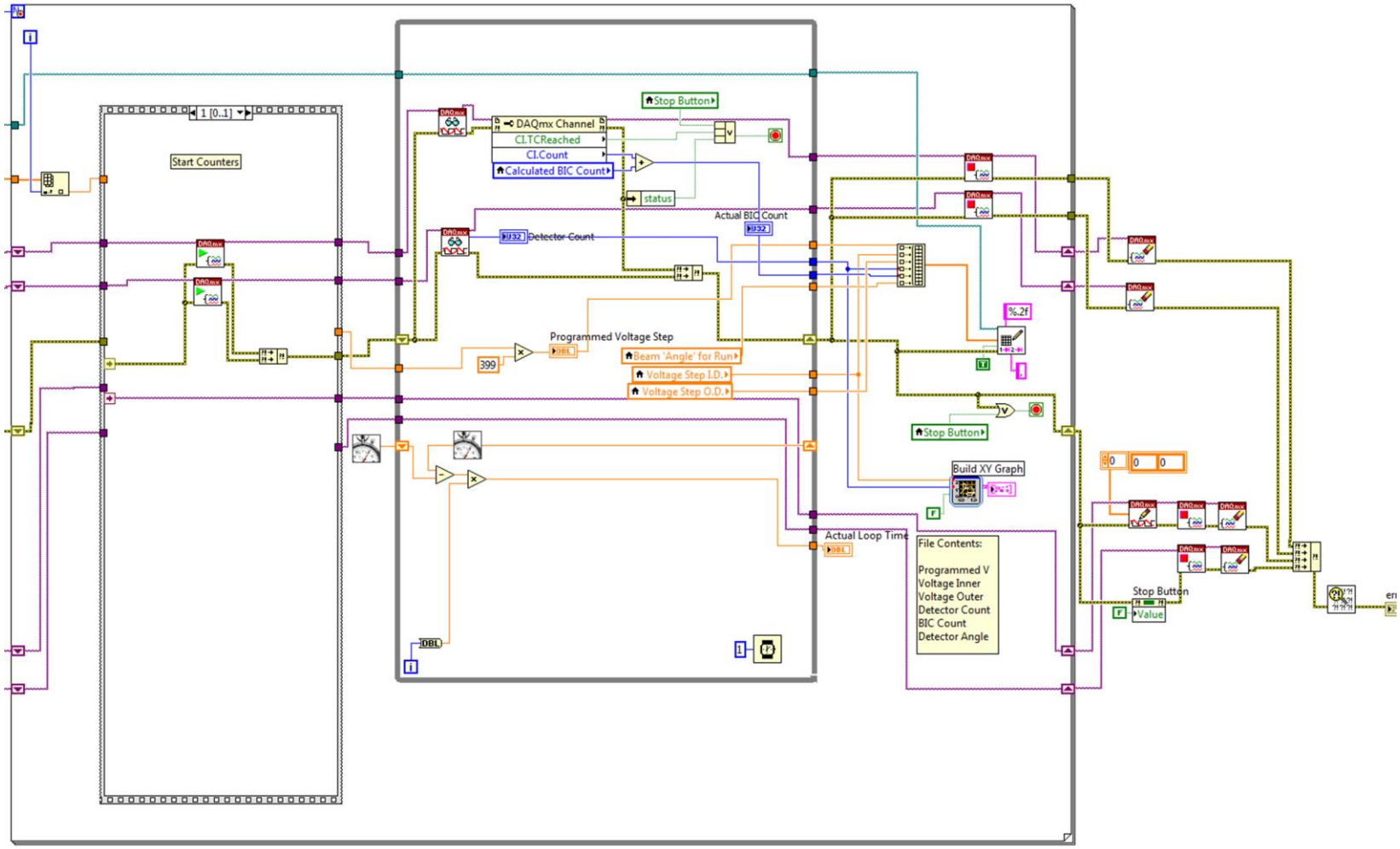

FIG 2.12 Block diagram of the LabVIEW run time loop with the second task of the first inner loop displayed. This task starts the counters built into the NI USB device for counting protons and electrons. The outer run time loop stores the desired data on a generated CSV file and updates the 2D plot on the interface for each voltage step iteration.

produce an output CSV file containing the desired experimental data including analyzer plate reported voltages, BIC counts, electron counts, and detector angle for each voltage step. The amount of charge collected by the BIC is determined by the user in the LabVIEW user interface window and is referred to as the 'bucket size'. A typical value of bucket size for the experiments done for this project is 2×10^{-6} coulombs. The BIC range set by a dial on the electronics rack is read by the USB controller and reported in the user interface window for verification. This combination of bucket size, BIC range, and beam current intensity determines the amount of time for a sweep during data acquisition. For example, if one selects 2×10^{-6} coulombs for the BIC range, a 1×10^{-6} coulomb bucket size, and has 500 nA of beam on target, the BIC sends a total of 500 signal pulses as it collects the 1×10^{-6} coulombs of charge, resulting in a 2 second step time. The user interface of the LabVIEW program includes a section for set-up parameters, run-time parameters, and a real time generated graphical representation of all prior steps during a sweep. The set-up parameters and run-time parameters windows are displays generated by the set-up and run-time loops in the LabVIEW block diagram.

The set-up parameters displayed include the BIC range, bucket size, calculated BIC count, initial BIC count, and initial run time. This display is generated in the first task of the inner loop of the set-up loop shown in Fig. 2.8. Starting the program requires the input of a user generated CSV file with a list of the desired voltage steps as well as choosing the desired bucket size for the sweep. Once this CSV is selected, an initial task is executed that controls the parameters of proton counting. This task displays the BIC range, bucket size, a calculated BIC count, and the initial loop time for this single iteration of collecting the desired charge to verify the program successfully completed the correct counting procedure. This procedure is shown in the second task of the inner loop of the set-up loop in Fig. 2.9. The third task of this inner loop, displayed in

Fig. 2.10, sets up the procedure for counting electrons withe the discriminator input signals. In this same task, a pop-up window is programmed to display after the completion of the set-up loop asking the user if the previously executed proton counting procedure was executed according to the desired set parameters.

After this initial set-up parameter loop has been executed, the pop-up window generated is displayed and prompts the user to allow the program to continue to the run-time loop. This permission step is executed in the second loop on the LabVIEW program following the set-up loop, shown on the right in Fig. 2.8-10. If the user chooses to allow the program to execute, this second loop will allow the passage of the digital signals to the run-time loop, shown in Fig. 2.11-12. This is the main operating subroutine for the program.

The run-time loop is set to execute these same set-up parameters defined by the first subroutine a number of times equal to the number of comma separated variables in the CSV file chosen by the user at the beginning of the run. During this time, a series of numbers are displayed in the run-time parameters area in the user interface. These numbers include the actual BIC count for the step, the detector angle, the programmed voltage of the step, the actual voltages of each analyzer plate read back through the USB controller, the actual loop time, and the detector count. The detector count is a constantly changing number showing the total accumulated electrons counted during the current voltage step. As the sweep is taking place, the run-time loop updates the automatically scaling graph in the user interface to display the previously calculated detector counts for each voltage step. This data is also saved as an output CSV file by the third subroutine simultaneously. This allows the user to notice trends or errors in the sweep as it happens to allow for more efficient troubleshooting. In case of an error, the program has been equipped with a stop function, displayed on the user interface that will end the

sweep and return all instruments back to 0 V in order to ensure proper shut down procedure. The first inner loop of the run-time loop consists of two tasks. The first task, displayed in Fig. 2.11, receives selected voltage step value from the input CSV file array corresponding to the numbered loop the run-time loop is on currently. This number, previously divided by 400 to scale the 0-2000 V high voltage power supply range to 0-5 V, is multiplied by 400 to report the power supply's actual voltage setting. This voltage step number is then recorded to an array with the number 10 to be later used to set the voltage input to the angle determining potentiometer. The detector angle is measured by applying 10 V to the potentiometer and reading a 0-10 V output signal. Also in this task are outputs designed to display the beam angle and analyzer plate voltages to the user interface. In the second task of the first inner loop of the run-time loop, displayed in Fig. 2.12, are two subroutines used to start the internal counters for proton and electron counting. The second inner loop in the run-time loop, shown in Fig. 2.11-12 on the right, is responsible for the counting and recording of electrons and protons. This loop iterates each time a signal is detected from the BIC until the BIC calculated count is reached. During this time, electron counts and BIC counts are updated in real time onto the user interface. Once the calculated BIC count is reached, this second inner loop stops, passes the collected BIC count, electron count, and loop time to the generated output CSV file and 2D graph display on the user interface. The actual loop time is calculated average of the second inner loop execution times. This second loop completing iterations equal to the calculated BIC count represents one voltage step. After this second inner loop finishes and the data is stored and reported, the run-time loop has completed one iteration then starts over for the next voltage step number on the list of the input CSV file. After the run-time loop has iterated a number of times equal to the number of

numbers in the input CSV file, the loop is completed, all controlled hardware is returned to 0 V operating potential, and the program ends.

The color coding system in LabVIEW offers organization and tracking methods for the programmer. The yellow lines shown in Fig. 2.8-12 are error routes, allowing the passage of an error message through the program to be reported at any stage of the program, regardless of when the program ends. The orange lines are analog signals, the blue lines are digital signals, and the burgundy lines are task propagations. Various subroutines used including those shown with glasses to read signals, those with pencils to write signals, etc. are built in functions of LabVIEW and are not shown.

2.4 Electron Gun

An electron gun was used prior to electron measurements with gas targets in order to test various components of the data acquisition system and the analyzers. A side-view schematic and electronic diagram of the electron gun are shown in Fig. 2.13. A potential difference of 4 V is applied to a 40 W light bulb filament and biased on one side with a high voltage supply. The 4 V bias on the tungsten filament ejects electrons off of the filament surface from thermionic emission [15]. The high voltage power supply biases the filament at a selected negative voltage in a range of 0-800 V, which creates a repulsive field to accelerate the now free electrons away from the filament. This bulb is housed in a collimating barrel that is insulated from the mounting platform to prevent a path to ground. The result is a beam of electrons in an energy range of the applied voltage to four less than the applied voltage times the elementary charge. The electron gun was initially used as a tool to test the new data acquisition system with the CMA that has a previously measured geometric coefficient, then later used to measure the geometric coefficient of the CDA. The electron gun was positioned at -70° with respect to the proton beam path, facing the analyzers that were positioned at 110° with respect the proton beam path. These experiments were conducted without the use of the proton beam from the accelerator, but instead with a NIST calibrated current source to electronically simulate a proton beam.

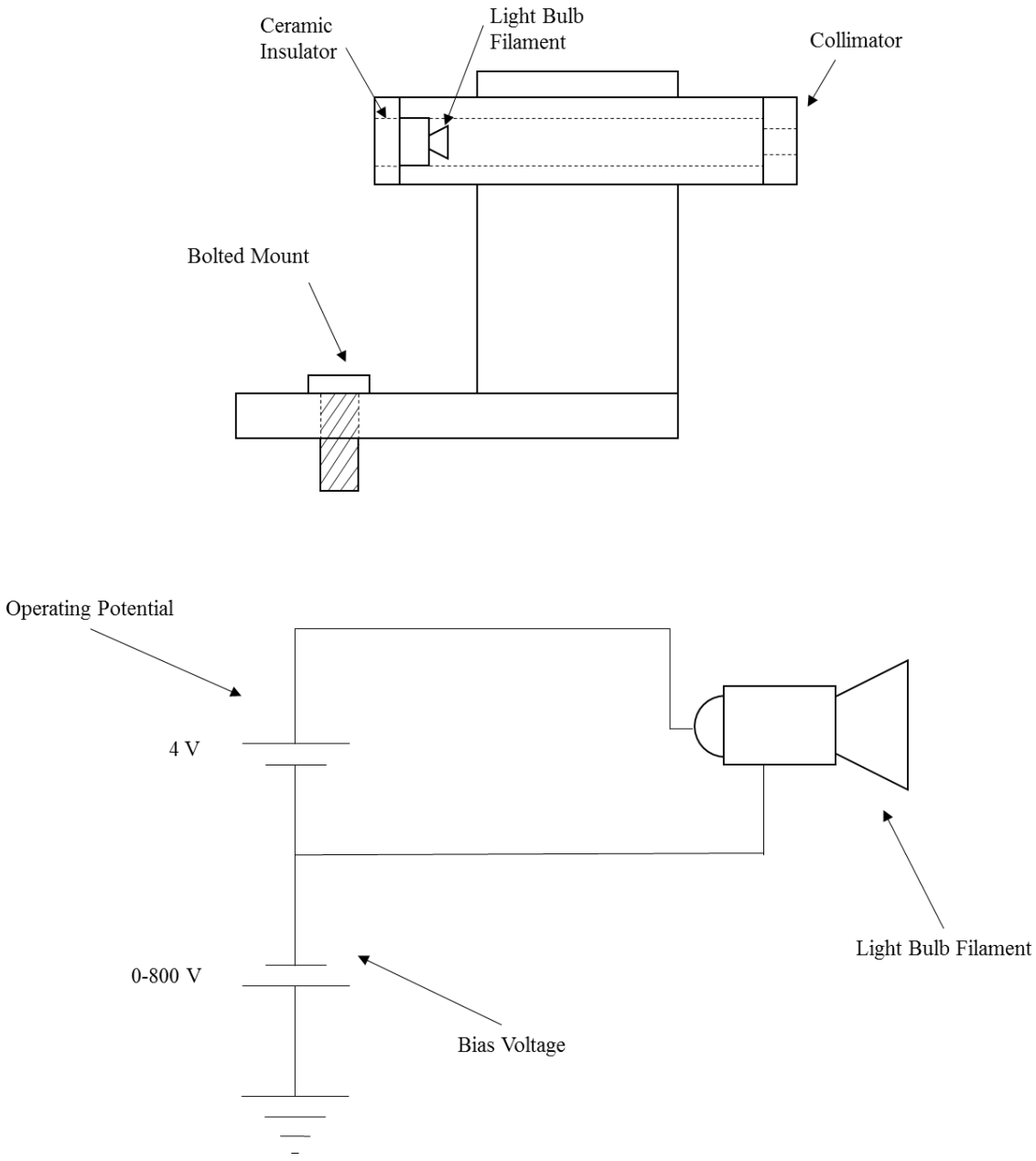

FIG 2.13 Schematics of the electron gun mounting apparatus and circuit designed for testing and calibration of the electron spectroscopy system.

3 Results and Discussion

3.1 CMA Data

Preliminary tests were conducted using the electron gun designed on site to confirm functionality of the analyzers used and the new data acquisition system prior to experimentation with gas targets. The first analyzer used was a cylindrical mirror analyzer. This analyzer was designed to have a geometric coefficient of 1 and measured to have a geometric coefficient of 0.98±0.02 by Moreau [11]. An early test was performed to check the functionality of the recently cleaned and refurbished CMA by biasing the electron gun at 245 V and running the LabVIEW program to sweep from 190-300 V in 5 V steps in order to establish a maximum in electron counts. This experimental data is shown in Fig. 3.1. As a second test of the CMA's angular acceptance limitations, the analyzer was rotated 2.5 degrees off of the electron gun's collimated beam path and the same sweep was run once more, also shown in Fig. 3.1. Even though the CMA electron gun tests were done with low resolution, a peak around 245 V was found, which supports the formally measured geometric coefficient.

After electron gun testing of the CMA and data acquisition system, the CMA was used to measure electron emission from gas targets to test the gas target system and compare to well-known electron emission information about select target gases. The gases used for testing the system were argon and neon. Auger-electron peaks were found by scanning the CMA voltage over ranges containing the known auger peak locations. The known auger emission electron energy for argon and neon are 205 eV and 815 eV respectively [16].

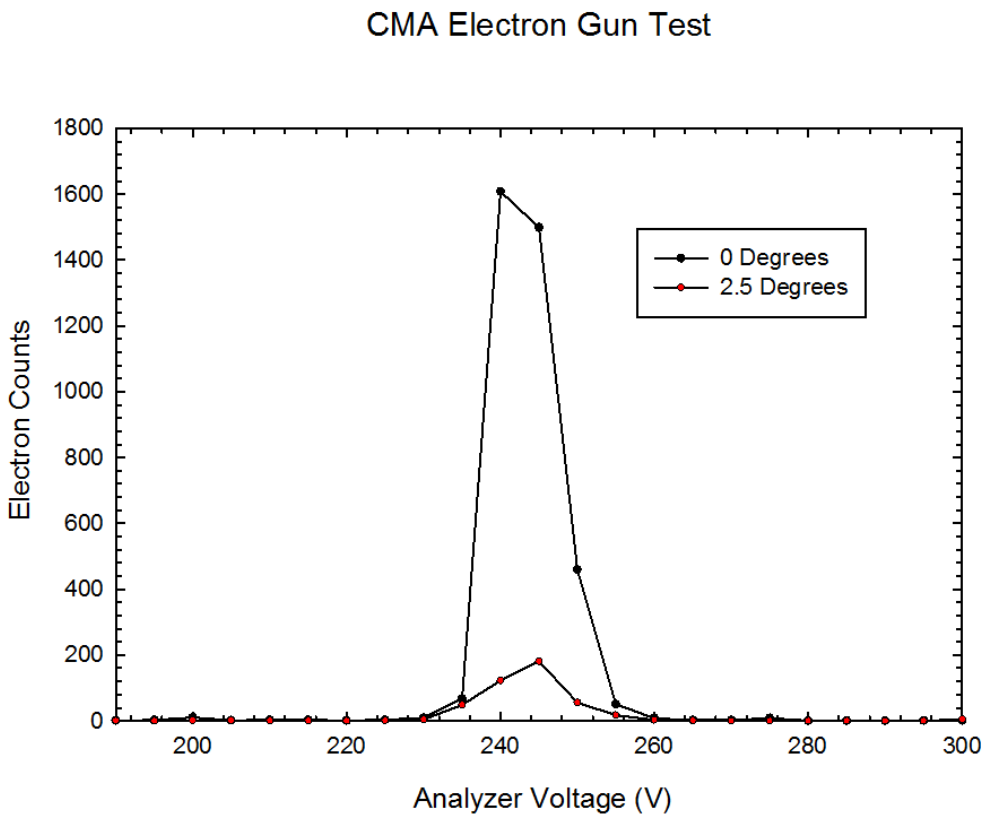

FIG 3.1 Graph of the CMA electron gun test. The electron gun was biased at 245 V. 5 V steps were taken between 190 V and 300 V. To test angular acceptance, the CMA was moved 2.5 degrees off of center to check for a lower count rate. Lines are to guide the eye only.

The first gas used for CMA testing was argon. The results from 2 MeV protons incident on argon gas is shown in Fig. 3.2. A tank of high purity argon gas was connected to the gas inlet system equipped with a pressure regulator. The regulator was used to set the gas output from the tank to be just over atmospheric pressure by a couple of pounds per square inch. The argon gas was injected via the collimated holes structure in a jet stream with a constant pushing pressure of 205 mTorr. This resulted in a chamber pressure of 1×10^{-7} Torr, up from a background pressure of 3.4×10^{-6} Torr. The ion gauge used for chamber pressure measurement was calibrated for nitrogen gas, so a correction factor of 1.29 must be used to find the actual pressure of the chamber by dividing the reported pressure by the gas correction factor. This gives an actual chamber pressure of 2.6×10^{-6} Torr. The BIC range was set to 2×10^{-6} coulombs with a bucket size set in LabVIEW of 2×10^{-6} coulombs. During the majority of the argon CMA experiments, the beam on target was roughly 500 nA. This resulted in a step time of roughly 4 seconds. Sweeps were made from 0-400 V in 5 V steps on the analyzer voltage. Electron counts were taken for four different angles with respect to the incident proton beam: 45, 60, 75, and 90 degrees. For each angle, two sweeps of background electron counts were made with no gas target. With the argon gas as a target, five sweeps of electron counts were recorded per angle. The displayed electron counts in Fig. 3.2 represent the average of the five gas-in sweeps minus the average of the background sweeps. Auger electrons were detected as a peak clearly shown between 200 V and 220 V as expected. An additional spectrum of argon gas is shown in Fig. 3.3, showing electron counts for a higher range of the analyzer voltage. In addition to the 0-400 V range swept with 5 V resolution, electron counts were also recorded for the 400-1500 V analyzer voltage range. The 400-1500 V electron counts shown in Fig. 3.3 are the average counts from three sweeps minus the average of two background sweeps in 25 V increments.

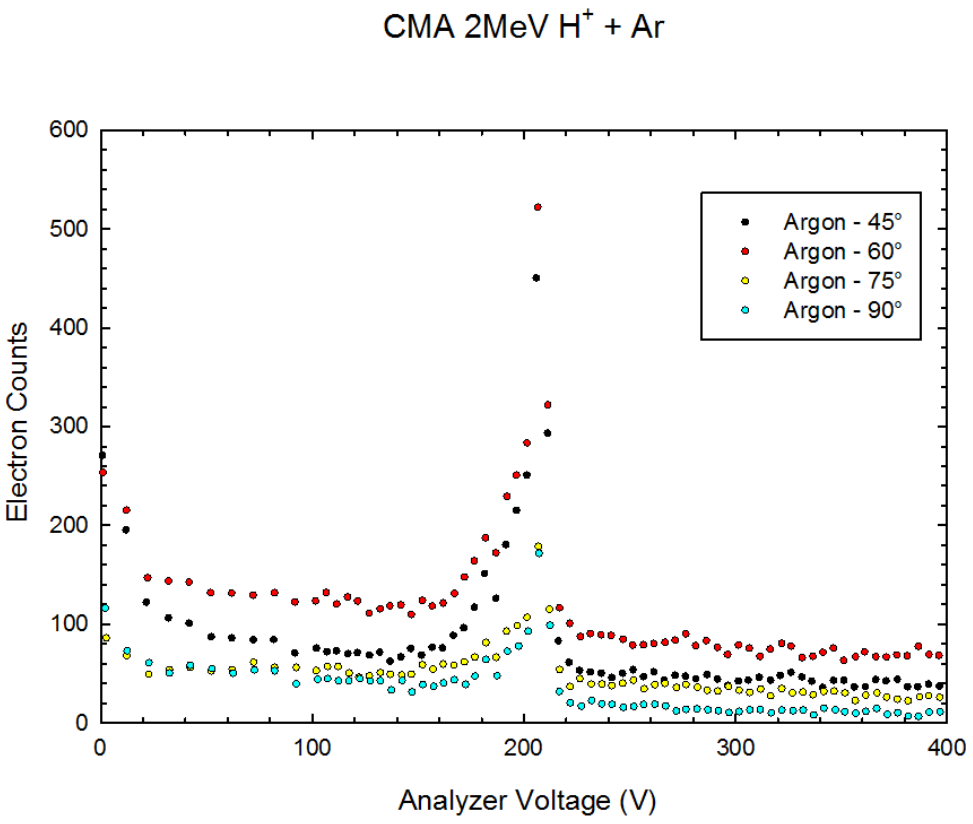

FIG 3.2 Plot of Ar K-Auger electrons taken with the CMA. The analyzer voltage was scanned from 0-400 V in 5 V steps. Electron counts were recorded for four different emission angles.

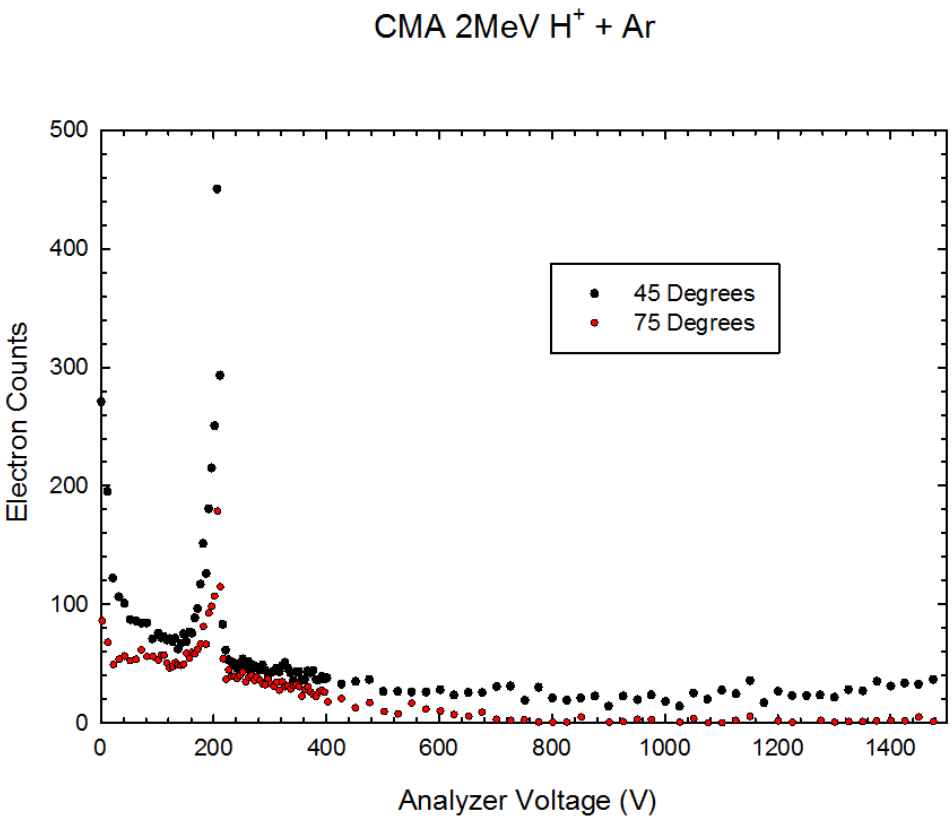

FIG 3.3 Plot of Ar K-Auger electrons including higher range 400-1500 V analyzer voltage taken with the CMA. Displayed are the 0-1500 V analyzer voltage range electron counts averaged and background subtracted for 45 degrees and 75 degrees angular position with respect to the incident beam.

While still using argon gas as a target, a variety of tests were conducted to verify the dependence of various parameters in the experiment. The parameters tested were the bucket size, pushing pressure of the target gas, and the absence of the magnetic shielding material. The results of these tests are shown in Fig. 3.4. To establish a control for these tests, the CMA was positioned at 45 degrees with respect to the incident proton beam for the entirety of the parameter variations with a gas target pushing pressure of 205 micro coulombs. Similar to the previous CMA argon experiment, the beam on target was roughly 500 nA for the entirety of the parameter test. Two background sweeps were also made for each parameter change and three sweeps taken for the given parameter. Similarly, the average of the parameter-changed sweeps was subtracted from the average background sweeps for the reported electron counts. To ensure that the measurements where linearly dependent on the bucket size, as would be expected, this parameter was doubled to 2×10^{-6} coulombs in the LabVIEW user interface. The result shown is a roughly doubling of the electron counts, verifying the data acquisition parameter. The gas target pushing pressure was also doubled from 205 mTorr to 410 mTorr to test the gas target density dependence. The expected result is a doubling of electron counts, and is seen in Fig. 3.4 as a roughly doubled value with respect to the control. Removal of the magnetic shielding was done to compare the effect of the presence of a magnetically unshielded target chamber on the spectrum. If external magnetic fields are at all altering the trajectory or the energy of scattered electrons, a possible change in peak height or peak shift may be expected. As shown in in Fig. 3.4, a small shift in the peak may or may not be arguable at this resolution.

A second target gas, neon, was selected in the testing of the CMA and data acquisition system to verify the operation of the gas inlet system for more than one gas. The results from 2 MeV protons incident on neon gas is shown in Fig. 3.5. A tank of high purity neon gas was

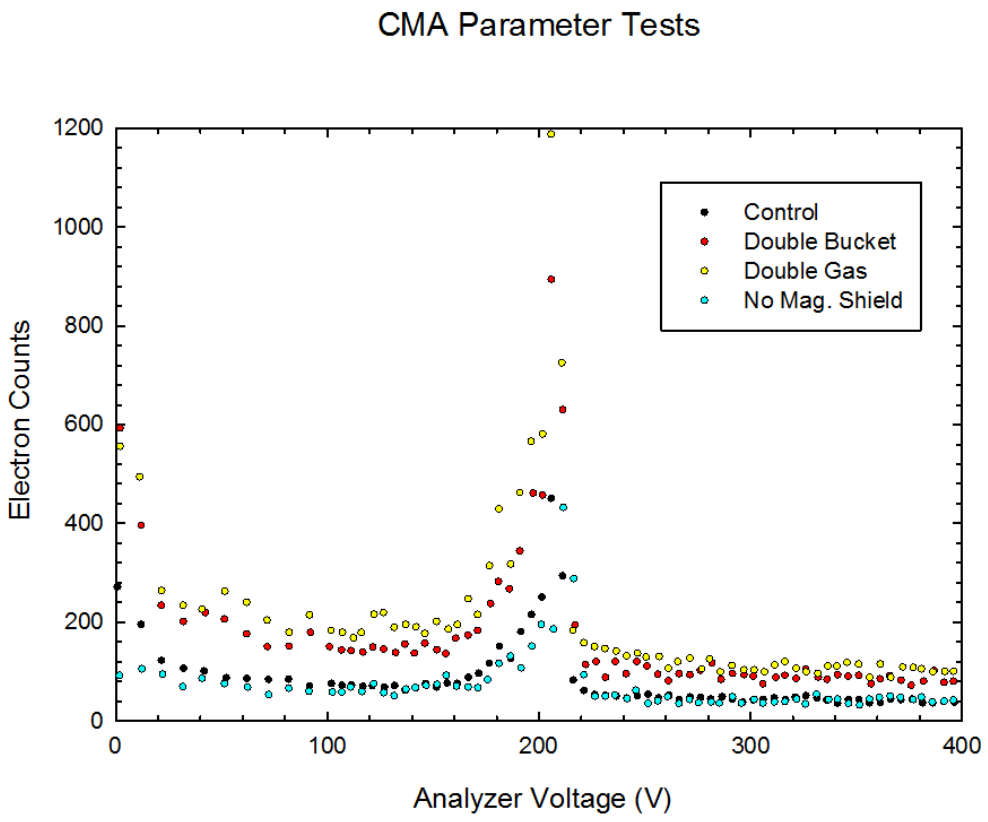

FIG 3.4 Plot of CMA parameter tests done with argon gas target. The analyzer voltage was scanned from 0-400 V in 5 V steps. Shown is a control data set and repeated data for different parameters including doubling the bucket size, the gas pushing pressure, and the absence of the magnetic shielding outside of the chamber. All data sets were taken at 45 degrees from the incident proton beam.

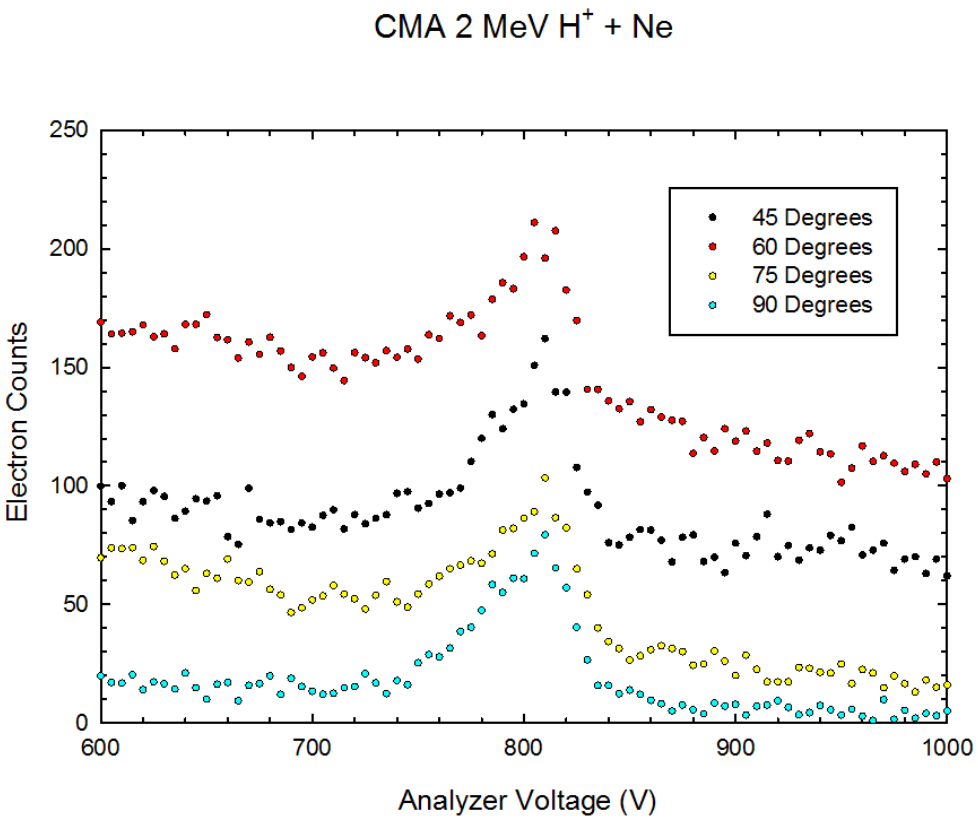

FIG 3.5 Plot of Ne K-Auger electrons taken with the CMA. The analyzer voltage was scanned from 600-1000 V in 5 V steps. Electron counts were recorded for four different angles.

connected to the gas inlet system. The neon gas was injected via the collimated hole structure in a jet stream with a constant pushing pressure of 650 mTorr. Similarly to the CMA argon experiment, this resulted in a change of the target chamber pressure from 1×10^{-7} Torr to a measured 2.8×10^{-6} Torr. With a gas correction factor for neon of .3 for the ion gauge used, the actual chamber pressure can be calculated to be 9×10^{-6} Torr. The BIC range was set to 2×10^{-6} coulombs with a bucket size set in LabVIEW of 2×10^{-6} coulombs. During the majority of the CMA neon experiments, the beam on target was roughly 500 nA. Sweeps were made from 600-1000 V in 5 V steps on the analyzer voltage. Electron counts were taken for four different angles with respect to the incident proton beam: 45, 60, 75, and 90 degrees. For each angle, two sweeps of background electron counts were made with no gas target. With the neon gas as a target, five sweeps of electron counts were recorded per angle. The displayed electron counts in Fig. 3.5 represent the average of the five gas-in sweeps minus the average of the background sweeps. Auger-electrons were detected as a peak clearly shown between 800 V and 820 V as expected. A noticeable difference in the data plotted in Fig. 3.5 is the high number of electron counts outside of the auger electron peak, relative to the peak height. This confusing issue was later explained by a discovery we made involving the gas inlet system. When the argon gas tank was replaced by the neon gas tank, the original regulator used remained on the argon tank and a new regulator was introduced. This new regulator was in fact not a pressure regulator but instead a flow rate meter. This unnoticed change lead to a series of problems with the gas inlet system. The process of letting gas into the target chamber involves, as mentioned before, setting the gas pressure from the tank to only a couple of pounds per square inch over atmospheric pressure. This was done by slightly increasing the regulator until the regulator pressure needle just left contact with the pin in the regulator gauge. After many repetitions of this

process during the CMA argon experiment, this process of just lifting the needle off of the gauge pin was done with the flow rate meter without noticing that a flow rate meter was being used. In hindsight, this explains why we had trouble maintaining what we thought was tank pre auto-leak valve pressure. The flow rate meter needle was constantly decreasing to touch the gauge pin, forcing us to continuously increase what we thought was pressure, but was actually flow rate after every few sweeps. The flow rate meter should in practice go to zero as it was doing because once the gas line was full of neon gas, the flow stopped. This was actually putting strain on the auto-leak valve by forcing it shut for the majority of the time during this experiment, only to open momentarily to allow more gas in the gas inlet system when the pushing pressure fell below the desired amount. During this momentary release of the auto-leak valve, we believe we were flooding the chamber with neon gas at a higher pushing pressure than desired, leading to a much higher target gas density that desired. As shown previously in Fig. 3.4, this unnecessarily large pushing and target chamber pressure should lead to higher electron counts at all ranges of electron energy. This is evident in the high level of electron counts for all values reported in Fig. 3.5. Due to time constraints and a complete redesign of the analyzer apparatus and wiring for the later installed CDA, this CMA neon data was unfortunately unable to be repeated.

3.2 CDA Data

After verification of the new data acquisition system and various components of the redesigned experimental target chamber functionality with the CMA that was used in the old system, a CDA was installed into the target chamber. This CDA was built at ECU by Dr. Toburen and Dr. McLawhorn prior to the lab renovation in 2011. Several modifications had to be made to incorporate the new analyzer including adapting the mounting apparatus, incorporating additional wiring, the installation of the channel electron multiplier salvaged from the CMA, and modifications to the LabVIEW program. Mounting adaptations were necessary to fit the CDA onto the rotatable arm in the target chamber, as well as mount the rotatable arm of the potentiometer to the CDA. The incorporation of an additional high voltage power supply and high voltage read-out was necessary due to the biasing of both inner and outer plates of the CDA, unlike the single outer plate biasing for the CMA. An additional port was used on the USB controller for both setting and reading the additional analyzer plate. Additional subroutines were added to the LabVIEW block diagram to control the extra voltage supply and read-out, as well as an additional display on the LabVIEW user interface.

The CDA used for this project was designed to have a geometric coefficient of .364. This coefficient is found by using the values of 1.25 inches and 1.5 inches for r_1 and r_2 respectively with Eq. 5. In order to determine the geometric coefficient experimentally using the electron gun, a series of sweeps were made by setting bias voltages on the electron gun ranging from 200-800 V in 25 V increments and plotted in Fig. 3.6. As the plot shows, at higher bias voltage the electron counts increased due to a higher energy electron beam being less scattered from self-repulsion. The important information obtained from the CDA electron gun calibration experiment displayed in Fig. 3.6 is the voltage of the center of the peaks produced at each mean

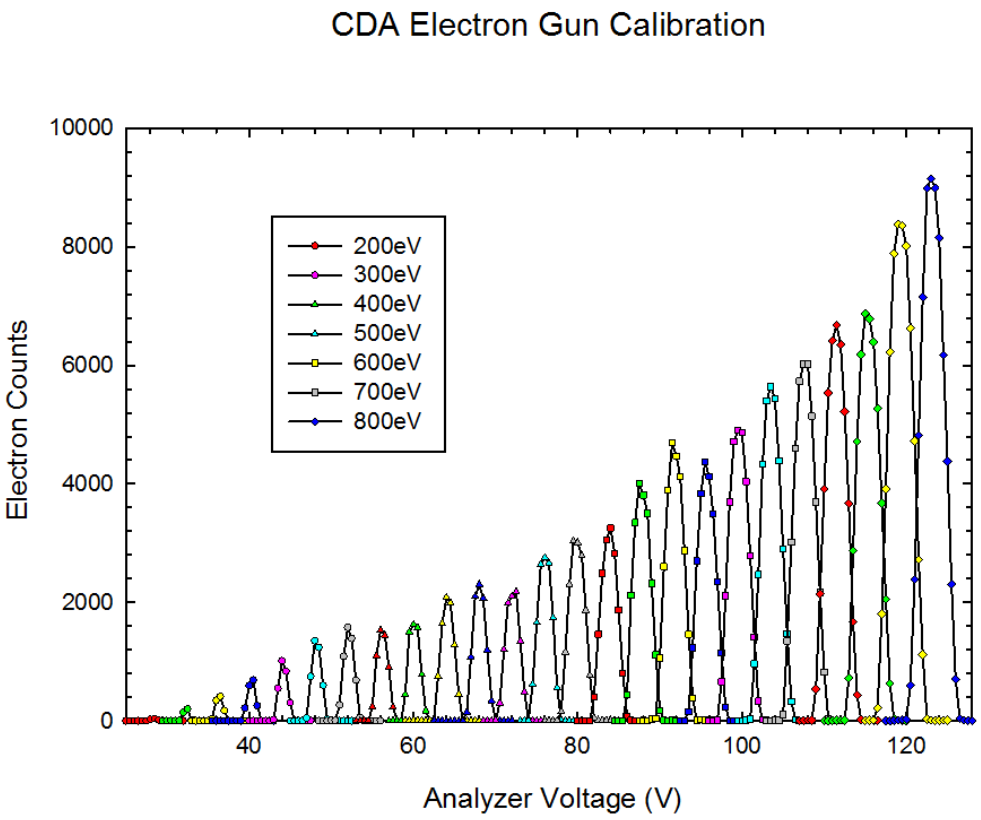

FIG 3.6 Plot of the CDA electron gun calibration. CDA was positioned 180° from the electron gun. The electron gun bias was set in 25 V increments from 200-800 V to create 200-800 eV electrons. Data was recorded in .5 V steps. Some electron energies are not shown in legend.

electron energy. The corresponding electron energies and analyzer voltage were plotted against each other to achieve a linear fit as shown in Fig. 3.7. Using a linear fit of the analyzer voltage and electron energies, the geometric coefficient of the CDA was determined not to be a simple coefficient as the slope of a best-fit line. The actual relationship between the analyzer voltage and electron pass energy is a linear relationship given by

$$V = .314E - 5.39 \quad (6)$$

The r^2 value for this fit was greater than .999. This experimentally measured geometric coefficient relationship was later used to verify functionality of the CDA with a gas target.

The final step in this experiment was to test the recently designed CDA with a new data acquisition system measuring electron emissions from a gas target in order to compare with previously measured data. We chose to use argon gas for this test as it was readily available from the prior CMA experiments. A plot of the electron counts is shown in Fig. 3.8. The previous procedures were repeated with a bucket size of 2×10^{-6} coulombs, BIC range of 2×10^{-6} coulombs, and gas inlet pushing pressure of 205 mTorr. The chamber pressure was reported to be 2.5×10^{-6} Torr corresponding to an actual chamber pressure of 1.9×10^{-6} Torr. During the majority of the CDA argon experiments, the beam on target was roughly 400 nA. Sweeps were made from 0-50 V in .5 V steps on each of the analyzer plates simultaneously at opposite polarities as described in chapter 1. This resulted in a sweep of 0-100 V in 1 V steps of the total analyzer potential difference, displayed in Fig. 3.8 as simply 'analyzer voltage'. Electron counts were taken for four different angles with respect to the incident proton beam: 45, 60, 75, and 90 degrees. For each angle, two sweeps of background electron counts were made with no gas target. With the argon gas as a target, five sweeps of electron counts were recorded per angle. The displayed electron counts in Fig. 3.8 represent the average of the five gas-in sweeps minus

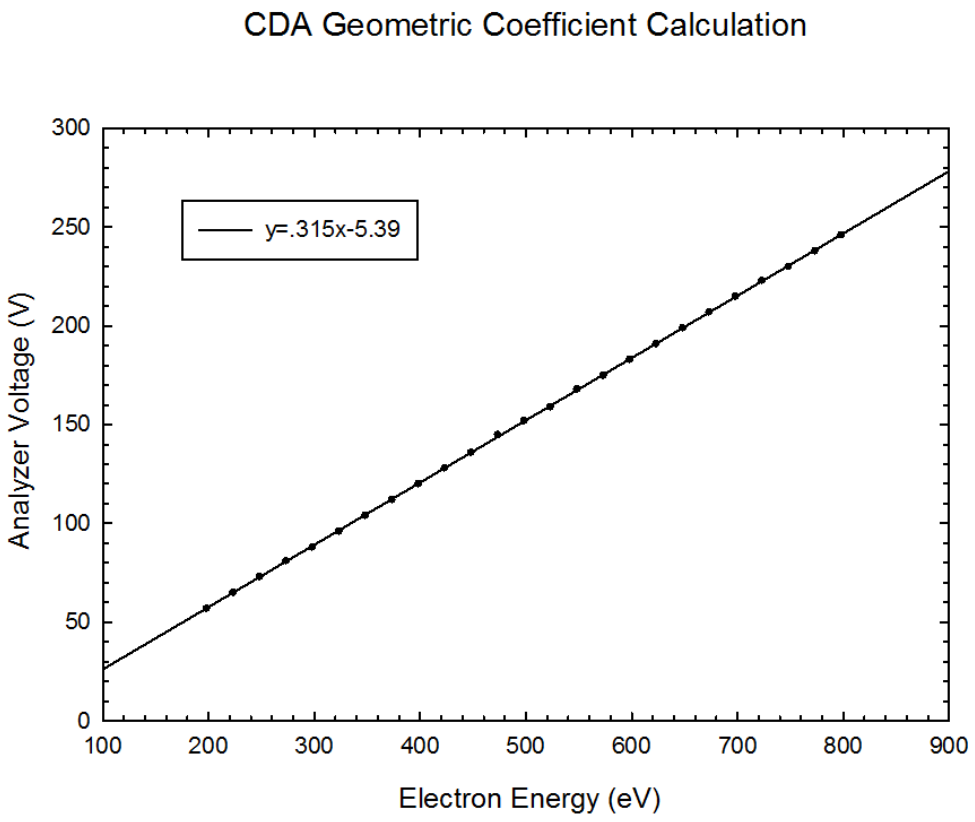

FIG 3.7 Plot of the CDA geometric coefficient calculation. The voltage of the center of each peak in the CDA electron gun calibration data set is plotted against the corresponding electron energy. The linear relationship between analyzer voltage and electron energy is shown in the legend.

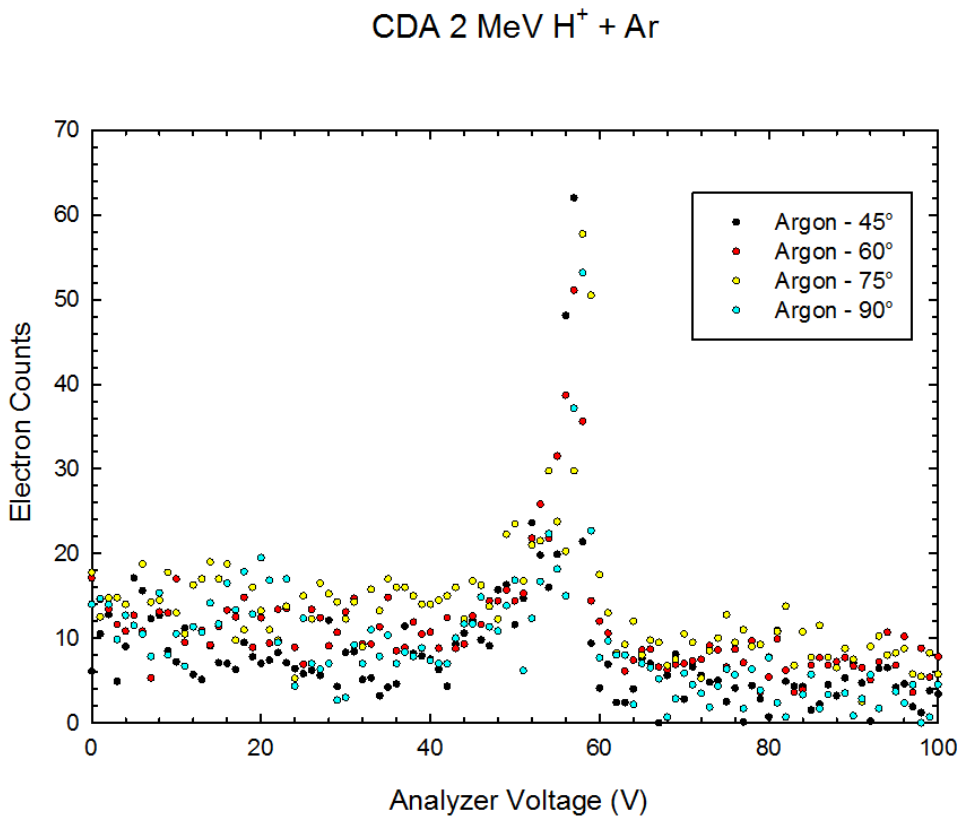

FIG 3.8 Plot of Ar K-Auger electrons taken with the CDA. The analyzer voltage was scanned from 0-100 V in .5 V steps. Electron counts were found for four different angles.

the average of the background sweeps.

Using Eq. 6 with known argon Auger-electron energy of 205 eV, we should find the auger peak at roughly 59 V. The peak shown in Fig. 3.8 lies between 55 V and 60 V as expected. This experiment verifies all components of the new data acquisition system with the CDA for detecting electron emission for gas targets. The electron counts for this experiment were considerably less than that of the CMA argon experiment. This is evidence of a smaller electron energy acceptance angle as predicted.

4 Conclusion

A new electron spectroscopy system was designed to measure electron emission from fast ion interactions. This spectroscopy system includes a new LabVIEW controlled data acquisition system and an ultrahigh-vacuum compatible cylindrical deflector analyzer (CDA). A preexisting cylindrical mirror analyzer (CMA) and target chamber designed for measuring electron emission cross sections were used to verify the operation of the new data acquisition system. The data acquisition system was successful in controlling the CMA and reproducing well-known K-shell Auger-electron emission data for argon and neon gas targets. Once the data acquisition system was operational, the new CDA was calibrated using an electron gun, then tested in the target chamber by reproducing the K-shell Auger-electron spectra obtained with the CMA. Upon completion of this project, the new CDA-equipped electron spectroscopy system will be moved to an ultrahigh-vacuum target chamber and used to measure high-energy electron spectra from fast-ion induced electron emission from condensed phase targets. These measurements using electrostatic analysis will extend the current low-energy electron emission spectra measured by electron time of flight to higher electron energies.

References

1. *Atomic, molecular, and optical physics : charged particles*, F.B. Dunning and R.G. Hulet, Editors. 1995, Academic Press: San Diego :.

2. Farnell, C.C., *Electrostatic analyzers with application to electric propulsion testing.* Proceedings of the 33rd International Electric Propulsion Conference (IEPC'13), 2013.

3. McLawhorn, R.A., *Electron Emission from Condensed Phase Targets Induced by Fast Protons*. 2008, East Carolina University.

4. Toburen, L.H., McLawhorn S. L., McLawhorn R. A., Carnes, K. D., Dingfelder, M., Shinpaugh, J. L., *Electron Emission from Amorphous Solid Water Induced by Passage of Energetic Protons and Flourine Ions.* Radiation Research, 2010. **174.1**: p. 107-118.

5. Simpson, J.A., *Design of Retarding Field Energy Analyzers.* Rev. Sci. Instrum., 1961. **32**: p. 1283.

6. Roy, D., and D. Tremblay, *Design of electron spectrometers.* 1990. **Rep. Prog. Phys. 53**(1621-1674.).

7. P. Bryce, R.L.D., J. C. Kelly, *The 127° Electrostatic Analyzer: Performance as a Spactrometer.* Canadian Journal of Physics, 1973. **51**: p. 574-586.

8. Beiser, A., *Concepts of Modern Physics*. 2003: Teta McGraw-Hill Education.

9. Stolterfoht, N., DuBois, R. D., Rivarola, R. D., *Electron emission in heavy-ion-atom collisions*. 1997, Berlin: Springer.

10. McGuire, G.E., *Auger electron spectroscopy reference manual : a book of standard spectra for identification and interpretation of Auger electron spectroscopy data*. 1979, Plenum Press: New York :.

11. Moreau, C.R., *K-shell ionization of fluorocarbon molecules by 2 MeV protons*. 1998, East Carolina University.

12. *Particles and nuclei : an introduction to the physical concepts*, B. Povh, Editor. 2004, Springer: Berlin ;.

13. Middleton, R., *A Negative Ion Cookbook.* 1989: University of Pennsylvania.

14. *Sputtering by particle bombardment*, R. Behrisch and H.H. Andersen, Editors. 1981, Springer-Verlag: Berlin ;.

15. Neil W. Ashcroft, N.D.M., *Solid State Physics*. 1976, Saunders College, Philadelphia.

16. Wagner, C.D., *Chemical shifts of Auger lines, and the Auger parameter.* Chem. Soc., 1975. **60**: p. 291-300.